OPTIMISATION OF ENERGY EFFICIENCY AND COMMINUTION PROCESS OF A SINGLE TOGGLE JAW CRUSHER USING DISCRETE ELEMENT METHOD

PETER NDUNG'U MWANGI

MASTER OF SCIENCE
(Mechanical Engineering)

JOMO KENYATTA UNIVERSITY OF AGRICULTURE AND TECHNOLOGY

2021

Optimisation of Energy Efficiency and Comminution Process of a Single Toggle Jaw Crusher Using Discrete Element Method

Peter Ndung'u Mwangi

A Thesis Submitted in Partial Fulfilment of the Requirements for the Degree of Master of Science in Mechanical Engineering of the Jomo Kenyatta University of Agriculture and Technology

2021

DECLARATION

This thesis is my original work and has not been presented for a degree in any other university.

Signature..... Date...../...../.....

Peter Ndung'u Mwangi

This thesis has been submitted for examination with our approval as university supervisors:

Signature..... Date...../...../.....

Dr. Onesmus Mutuku Muvengei, PhD

JKUAT, Kenya

Signature..... Date...../...../.....

Dr. Thomas Ochuku Mbuya, PhD

UoN, Kenya

DEDICATION

I am dedicating this thesis to two beloved people who have meant and continue to mean so much to me. First, to my dear mother, Ng'endo, who has continued to guide and encourage me through my years of study. Second, to my wife, Nyagacu, the most wonderful, caring, loving and supportive woman who has been my strength during difficult times.

ACKNOWLEDGMENT

My greatest gratitude goes to God who has given me protection and strength throughout my study. I am also very grateful to my supervisors, Dr. Onesmus M. Muvengei and Dr. Thomas O. Mbuya for their supervision and tireless assistance throughout my study period. I as well thank Research, Production and Extension Division (RPE) and Jomo Kenyatta University of Agriculture and Technology (JKUAT) for sponsoring me financially during the study. I also appreciate Dr. Jackson Githu, Mr. Evans Kibiru, Eng. Mathew Ndeto and Mr. Joseph Kimani who have been of great assistance during the research period. My final thanks goes to my fellow Mechanical Engineering postgraduate students, and all my well-wishers.

TABLE OF CONTENTS

LIST OF TABLES

LIST OF FIGURES

LIST OF APPENDICES

LIST OF ABBREVIATIONS

ANFIS :Adaptice Neuro-Fuzzy Interference System

ANSYS :Analysis System

BPM :Bonded Particle Model

CAD :Computer Aided Design

DEM :Discrete Element Method

EDEM :Experts in Discrete Element Modelling

FBM :Fast Breakage Model

FEM :Finite Element Method

PRM :Particle Replacement Model

LIST OF SYMBOLS

β	Ratio of set to mean size of feed material
ϵ	Coefficient of restitution
ε	Strain Energy [J]
η	Efficiency [%]
γ	Fracture surface energy [J/m^2]
μ	Relative velocity [m/s]
ν	Poisson‘s ratio
ρ	Density [kg/m^3]
$\sigma_{x,y,z}$	Stresses along x, y and z axes respectively [Mpa]
θ	Nip angle [rad]
v	Frequency [rpm]
v_c	Critical frequency [rpm]
a, b, c	Semi-major axes of elliptical particles [mm]
C_n, C_t	Damping coefficients of normal and tangential forces respectively [Ns/]
D_n	Diameter of nth particle [m]
E	Young's modulus [Pa]
E_0	Threshold elastic strain energy [J]
F_{80}	Feed size in microns at which 80% passes through the sieve[μm]
F_n, F_t	Normal and tangential forces respectively [N]
F_r	Dimensionless surface roughness factor that corrects for non-sphericity [$1 \leq F_r \leq 3$]
G	Gape [m]
K	constant related to machine parameters
L	Height of jaw crusher [m]

L_{MIN}	Closed set [m]
L_{MAX}	Open set [m]
L_T	Throw [m]
k	Stiffness [N/m]
m	Mass [kg]
n	frequency of strokes per minute [rpm]
P_K	Size distribution function or packing characteristics
P	Load [N]
P_{80}	Product size in microns at which 80% passes through the sieve[μm]
Q_A	Actual jaw crusher capacity [t/h]
Q_M	Maximum jaw crusher capacity [t/h]
R	Reduction ratio
S	Tensile strength [Pa]
S_c	Parameter related to rock surface characteristics
S_f	Surface area of feed particle [m^2]
S_p	Surface area of product particle [m^2]
W	Work input [kWh t^{-1}]
W_i	Bond's work index [kWh t^{-1}]
Y	Elastic strain energy [J]

ABSTRACT

Jaw crushers are considered among the primary crushers in mining industry. The size reduction process, also known as comminution, is not only an energy intensive process but also energy inefficient. There have been numerous attempts which aim at optimising the energy efficiency of jaw crushers. For instance, the use of chemicals to induce cracks before the breakage has been suggested but that process raises the overall cost of aggregate production. The main objective of this research is to optimise the energy efficiency of a single toggle jaw crusher using Discrete Element Method (DEM). DEM was employed in prediction of the energy consumption of the jaw crusher for different operating parameters. In a jaw crusher, the throw, reduction ratio and toggle speed frequency are very critical to energy consumption. These parameters were varied according to the guidelines used by jaw crusher manufacturers and which have also been validated by researchers. Simulation of the comminution process requires modelling of feed material. In this work, modelling of the feed material (rocks) was carried out using EDEM Academic software. The Bonded Particle Model (BPM) was selected as the technique for modelling the rocks due to its superlative features, in comparison to Particle Replacement Model (PRM) and Fast Breakage Model (FBM). For instance, in BPM, the particle dynamics are retained after breakage unlike in PRM and FBM where broken particles are replaced by new ones. In addition, an irregular shaped rock particle was created using the custom Application Program Interface (API) feature in EDEM software. The use of API required coding using C++ language which in turn made it possible for custom factories to be created. The wear distribution along the jaw crusher liners was also investigated using EDEM software. The wear distribution was depicted using the Relative Wear feature in EDEM software. The energy efficiency was calculated from new surface area created from fracture of the BPM rock. The results were fed into MINITAB software which developed the regression model showing the relationship between energy efficiency, throw, reduction ratio and toggle speed frequency. A Genetic Algorithm was used to obtain the optimal energy efficiency. The optimal energy efficiency was obtained as 59.778% at a throw of 35 mm, reduction ratio of 4 and a toggle speed frequency of 160 rpm. There was a great improvement in energy efficiency of the single toggle jaw crusher in comparison to the 6.023% efficiency of the un-optimised jaw crusher. In addition, conventional designs have efficiencies of less than 10% and hence the results obtained in this research have shown that maximisation of energy efficiency is possible. During the comminution process, it was observed that throw, reduction ratio and toggle speed have different levels of impact on the energy efficiency. The throw and reduction ratio were found to have a higher impact on energy efficiency than the toggle speed frequency. Wear distribution was also prominent near the Close Side Set (CSS) of the jaw crusher.

CHAPTER ONE

INTRODUCTION

1.1 Background

Worldwide, mineral mining plays a vital role in economy growth, and maintaining and improving the quality of life and functioning of the modern society. Mineral ores are often massive in size and they need to be broken down into smaller sizes (Khanal, 2005). Minerals normally exist in chemical and physical combinations with each other and hence, to separate minerals of commercial interest from the ore, both physical and chemical processes are employed. Therefore, for these minerals to be accessible, the ores have to be crushed or even ground. The process of reducing the size of large and hard ores is known as comminution. Comminution can be executed by either application of pressure, impact force or a combination of both (A. Gupta & Yan, 2006).

Comminution is a very inefficient and energy demanding process. This is mainly due to random application of forces inside the machine and also due to inter-particle collisions. The applied forces for comminution are translated to heat, noise and elastic particle deformation which results in energy losses of up to 90% (Legendre & Zevenhoven, 2014). Even though so much work has been done in the area of size reduction (Donovan, 2003), most researchers have put more emphasis on quality of particle size distribution rather than minimising the power consumption (Legendre & Zevenhoven, 2014).

In Kenya, the stone crushing industry is not only an indicator of the progress of the nation but is also a great contributor to her growth. For instance, as of 2018

the value of completed buildings in Kenya registered a growth of 10.2% and formal employment in the sector grew by 11.4% (NCA (National Construction Authority), 2018). According to the Trading Economics, the gross domestic product (GDP) from construction increased from KES 67.637 Billion to KES 74.790 Billion between July 2018 and January 2019 (*Kenya GDP From Construction*, 2019). This has shown that the demand for aggregate production will only increase. However, in developing and middle income countries, the stone crushing industry is characterized by few large-scale and centralized stone crushers and hundreds of small scale stone crushers. Therefore, to ensure that small-scale entrepreneurs gain from construction industry, there is need for an affordable comminution machine (Munyasi & Oduori, 2013).

Manual stone crushing is not only inefficient but is also hazardous to human health. The high demand for aggregates in Kenya has forced many people in both urban and rural areas to resort to manual stone crushing as a means of earning livelihood. In rural areas, the transportation costs of aggregates from the crushing point to buyers often costs more than the price of aggregates. Some of the tools used in aggregate production include; sledge hammers, wheelbarrows, anvil, etc. Such tools are not safe to humans especially children who also take part in manual stone crushing (Munyasi & Oduori, 2013).

There are many factors which constrain Kenyans from improving their economic status while relying on manual stone crushing. Men and women who produce aggregates manually are exposed to high risk due to body injuries, inhalation of dust, exposure to harsh weather conditions and lack of proper transport system from quarries to crushing site. In addition to being dangerous, manual stone crushing yields low quantity and inferior products (Munyasi & Oduori, 2013). To eliminate this problem, a group of researchers and innovators presented a proposal to the Research, Production and Extension (RPE) division of JKUAT to develop a small scale jaw crusher as shown in Figure 1.1. The proposed jaw crusher would be

accessible to small scale stone crushing enterprises and entrepreneurs who would be willing to produce about 15 wheelbarrows of aggregate a day. The dimensions and process parameters of the preliminary jaw crusher design are as shown in Table 1.1. The need for a better means of producing aggregates is inevitable. Jaw crushers

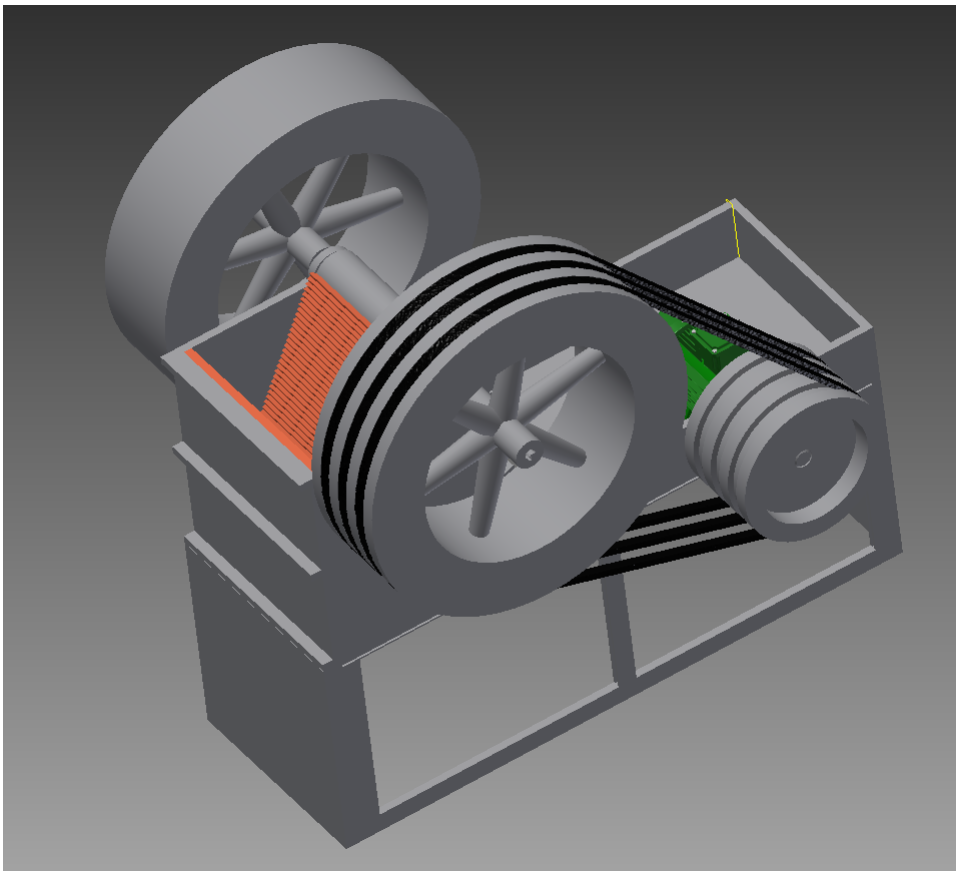

Figure 1.1: Preliminary design of the jaw crusher

are mechanical machines which are used for comminution process in quarries. These robust machines are used in both large scale and small scale industries. Large scale stone crushing industries rely so much on mechanically operated equipment such as gyratory crushers, roll crushers and jaw crushers. Roll crushers and gyratory crushers operate primarily by the application of impact force while jaw crushers are basically compression crushers. Stone crushers come in various capacities and sizes ranging from 0.2-50 t/h (Deepak, 2010).

Table 1.1: Parameters and dimensions of the preliminary design of the jaw crusher

Parameter	Dimension	Unit
Gape	0.235	m
Width	0.47	m
Length	0.5	m
Throw	0.035	m
Reduction Ratio	3	-
Toggle speed	200	rpm

1.1.1 Jaw Crusher Design

Jaw crushers are machines designed to impart compression and impact forces on a rock placed between two plates. In a jaw crusher, one of the plates moves (swings) while the other one remains stationary (fixed). Liners made of hardened steel are usually fixed on the jaws. These liners can be both flat or convex or a combination of both (Suresh, 2009). There are two main types of jaw crushers; Blake jaw crushers and Dodge jaw crushers.

i. Blake Jaw Crushers

In Blake jaw crushers, the swing jaw is pivoted at the top of the frame so as to attain a maximum amplitude at the bottom of the crushing jaws. Usually, Blake crushers are controlled by the pitman and operated by toggles. The size of the opening feed is known as the 'gape' while that of the closing feed is known as the 'set'. Blake jaw crushers can be single-toggle or double-toggle (Deepak, 2010).

Single Toggle Jaw Crusher

This type of crusher has only one toggle plate as shown in Figure 1.2 (a). It has less weight and is cheaper in comparison to the double toggle type.

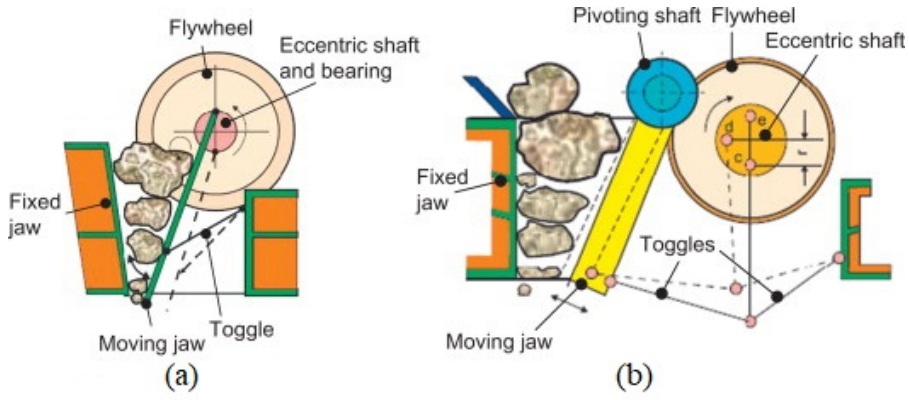

Figure 1.2: Single toggle (a) and double toggle (b) jaw crushers (Suresh, 2009)

Double Toggle Jaw Crusher

This crusher has two toggle plates as shown in Figure 1.2 (b). Even though the double toggle jaw crusher crushes tough and abrasive rocks, it is heavier and costly to manufacture.

Blake type jaw crushers are very popular due to the following reasons:

- They are easy to repair and simple to adjust so that minimal wear is experienced during operation.
- They are able to crush blocky and abrasive rocks.
- It is possible to reinforce the crusher using a high strength crusher frame. This makes them ideal for crushing very hard rocks.

ii. Dodge Jaw Crushers

In these jaw crushers, the moving jaw is pivoted at the bottom and connected to the eccentric shaft. The movable jaw is hinged at the bottom of the crusher frame to ensure that maximum amplitude if motion is at the top of the jaws as shown in Figure 1.3. These crushers are commonly used in laboratories due to their small capacity (Deepak, 2010).

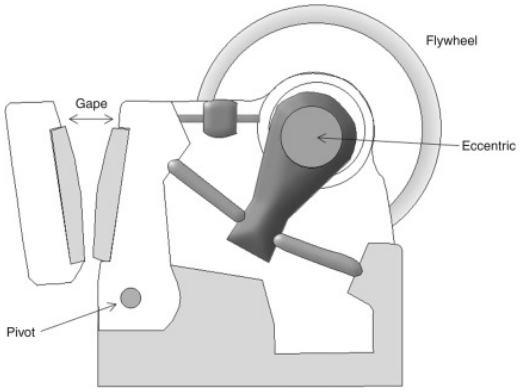

Figure 1.3: Dodge type jaw crusher (Deepak, 2010)

1.1.2 Components of a Jaw Crusher

Swing Jaw:

This is the main moving part of a jaw crusher. Its movement is achieved through the eccentric shaft which provided enough force to crush the rocks.

Fixed Jaw:

It is located on the opposite side of the pitman and is statically mounted. It is covered with liners which prevent it from wear.

Liners:

Jaw crusher liners are made of hardened manganese steel. They are usually symmetrical at the top and flipped over at the bottom as most wear takes place at the closed side of the jaw crusher. Liners are mounted on the crushing side of both the fixed jaw and swing jaw.

Toggle Plate:

The toggle plate acts as a fail-safe device in the jaw crusher. If a non-crushable material which is larger than the closed side setting, the toggle plate will crush in order to prevent further damage to the jaw crusher. A good example of a non-crushable material is the steel loader tooth or the tramp iron which are present in mined rock debris.

Eccentric Shaft:

This provides the eccentric motion of the swing jaw. It goes through the entire length of the swing jaw.

1.2 Problem Statement

For many years, comminution has always been associated with low efficiency rates. This is probably because a majority of designers have been interested in the particle size rather than energy consumption (Deepak, 2010).

According to Legendre (Legendre & Zevenhoven, 2014), only 10% of the energy input is used for size reduction during comminution. The dissipative nature of comminution processes is as a result of random application of forces inside the machinery and between neighbouring particles. Machine parameters such as shaft velocities, geometry, particle size and material properties affect the overall efficiency of a jaw crusher. However, models that take into account all the variables affecting a jaw crusher's performance are difficult to find. Another approach would be to change the rock's material property before the crushing process commences (Tromans, 2008). However, material pre-treatment techniques that will destabilize the rocks internal structure will require more resources such as energy and capital which might not be available to a small scale miners.

Comminution machines are not only inefficient but are also too expensive for small scale miners. This implies that only well-established firms/industries can afford to exploit the mining industry hence forcing upcoming entrepreneurs to rely on manual stone crushing as a source of livelihood. An optimised single toggle jaw crusher will improve quality and quantity of aggregates. A small scale jaw crusher will also eliminate transport costs and increase production from 0.014 ton per hour to 0.2 ton per hour (Munyasi & Oduori, 2013).

Discrete Element Method (DEM) has not been fully utilised in energy efficiency optimisation for jaw crushers. Legendre (Legendre & Zevenhoven, 2014) used DEM to assess the energy consumption of the jaw crusher but not the optimisation of comminution. DEM is a sophisticated method for the analysis of fracture of discrete elements which demands high computational power. In addition, Finite Element Method (FEM) has been used by researchers in wear analysis of liners during comminution. While FEM is a good tool for wear analysis, it is not applicable for discrete matter such as rocks.

1.3 Objectives

The main objective of this research project is to optimise the design of a single toggle jaw crusher, for improved comminution process, energy efficiency and power consumption. To achieve this, the following specific objectives were accomplished:

1. Develop a validated Discrete Element Model of the stone crushing behaviour by a single toggle jaw crusher in order to assess the energy consumption of the crusher.
2. Estimate the wear distribution of the jaws during the comminution process.
3. Identify the process parameters that have an impact on energy efficiency of the jaw crusher.

4. optimise the energy efficiency and power consumption of a single toggle jaw crusher during the comminution process.

1.4 Justification

Construction industry is one of the most lucrative and fastest growing investment in Kenya. A decade ago, the demand for aggregates was not as high as today and the numbers will increase in the near future. However, aggregate production is an industry which is only for big industries or entrepreneurs who can afford the massive jaw crushers. For instance, the price of single toggle jaw crushers in Kenya start from Ksh. 500,000 with an average capacity of 1 - 1.5 t/h. This creates a room for monopoly in which only big corporations can produce huge quantities of aggregates.

In addition to having massive jaw crushers in quarries, Kenyans in rural and urban areas have opted for manual stone crushing. Use of sledge hammers and anvil to crush stones and wheelbarrows to transport aggregates from crushing sites is hazardous to human health. During manual stone crushing, the dust generated affects men, women and children and might lead to asthmatic conditions. Injuries are also inevitable in manual stone crushing process.

Manual stone crushing process results in low quality and low quantity aggregates. For instance, a hard-working man and woman will take 3 weeks and 4 weeks respectively to produce 7 tons of aggregates while a single toggle jaw crusher will produce at least 100.8 tons of aggregates in 21 days. The quality of aggregates from manual stone crushing is not always consistent as a man's productivity deteriorates during working hours.

This gives the need for a small scale jaw crusher. A double toggle jaw crusher is heavier and more costly to fabricate hence making it unsuitable for small scale entrepreneurs. On the other hand, a single toggle jaw crusher is cheaper to fabricate

and is lighter in weight than the double toggle type. A small scale jaw crusher will open doors of investment to small scale entrepreneurs. In addition, it will eliminate the hazardous conditions arising from manual stone crushing. Mechanized stone crushing will also yield high quality and high quantity of aggregates. This will highly improve Kenyan economy. Lastly, a small scale jaw crusher will reduce transportation costs as it can be easily transported to crushing sites.

Even though a small scale single toggle jaw crusher is more convenient in comparison to manual stone crushing, the comminution process is very energy inefficient. Therefore, the need for an optimisation process is inevitable. Using Discrete Element Method to assess the energy efficiency of the jaw crusher will give realistic results unlike Finite Element Method which only deals with continuum matter. Furthermore, the regions experiencing high wear rates during comminution will be established using DEM.

1.5 Organisation of the Thesis

This thesis is composed of five themed chapters:

Chapter 1 is the introductory chapter. Here, the relevant background information related to jaw crusher structure and performance is provided. The problem statement, objectives of the research and justification are also presented in this chapter.

Chapter 2 provides the literature review on jaw crusher energy consumption, optimisation of the comminution process, Discrete Element Method and Genetic Algorithms. In addition, the identified research gaps have been stated in this chapter.

Chapter 3 is the methodology chapter. The steps involved in creating the rock model using discrete element have been clearly outlined. In addition, the procedure for jaw crusher modelling, optimisation of the comminution process, estimation of the wear on liners and validation of results is present in this chapter.

Chapter 4 provides the results obtained from simulations. The objective function

for optimisation is presented in this chapter. In addition, the effect of the process parameters on energy efficiency and the optimised process parameters are available in this chapter. Wear distribution and interaction between the rock model and jaw crusher liners are done this chapter.

Chapter 5 is the conclusion and recommendations chapter. Here, the findings of this research work are provided and recommendations for future research have been provided.

CHAPTER TWO

LITERATURE REVIEW

2.1 Overview

Comminution in a jaw crusher is an energy intensive process which is characterised by low efficiencies. A huge percentage of the energy lost during comminution is brought about by vibration, friction and noise. Improving the energy efficiency can be done by either optimising the operational parameters or inducing flaws in the ore using chemical pre-treatment before crushing starts. The latter process is costly and will result in usage of more energy (Legendre & Zevenhoven, 2014). Researchers have worked on minimising the energy consumption of the comminution process but none has worked on optimising the operational parameters. In addition, there are high wear rates along the liners of the jaw crushers. While most work has been done on minimising the wear rate on the jaw crusher liners using Finite Element Analysis, little investigation has been conducted using Discrete Element Method. This chapter, therefore, presents a review of what has been achieved by researchers in analysing energy efficiency and wear distribution of the single toggle jaw crusher.

2.2 Jaw Crushers

Jaw crushers and gyratory crushers are the most commonly used machines in primary crushing. Primary crushing simply implies that the feed material is fed to the comminution machine directly from the blast site. This is the first stage of comminution. In primary crushing, large amounts of energy are required due to the significant amount of size reduction taking place. Rather than the size reduction process, the energy demand is subject to the quantity of materials being crushed,

the type of machine used and physical properties of the material (Khanal, 2005).

Breakage force in primary crushers is either compression or impact. Gyratory crushers are classified as impact crushers while jaw crushers are compressive crushers. In compressive crushing, the applied force is applied at a slower rate in comparison to impact crushing. This results in cleavage and abrasion fracture. Therefore, the rate of energy input is lower than in impact crushers as shown in Figure 2.1. Impact crushers are also known to have higher reduction ratios than compressive crushers but incur high rates of abrasive wear. This makes jaw crushers long lasting because of reduced wear.

Researchers have found that there is sufficient evidence that links energy consumption of a comminution machine to the rock properties (Deepak, 2010; Legendre & Zevenhoven, 2014; Zhang, 2016). These properties include particle tensile strength, fracture toughness and specific breakage energy. In accordance to Weibull's weakest link theory, the particle size also determines the amount of applied breakage energy (Donovan, 2003).

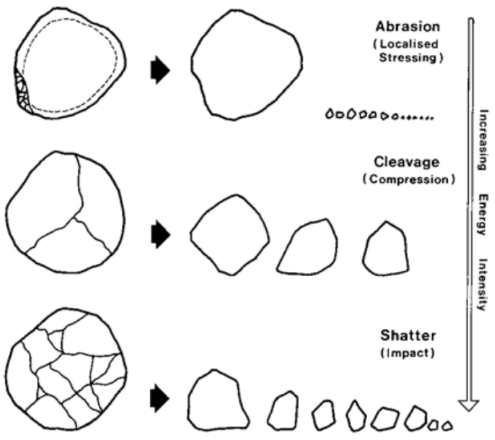

Figure 2.1: Abrasive, cleavage and shatter fracture (Donovan, 2003)

In jaw crushers feed material moves down the crushing chamber due to gravitational force as shown in Figure 2.2. Since the size of the crushing chamber decreases from

the gape to the set, the feed material is nipped by the swing jaw and is crushed before moving to the next crushing zone. The crushing process continues until the material average diameter is equal or less than the size of the set (A. Gupta & Yan, 2006).

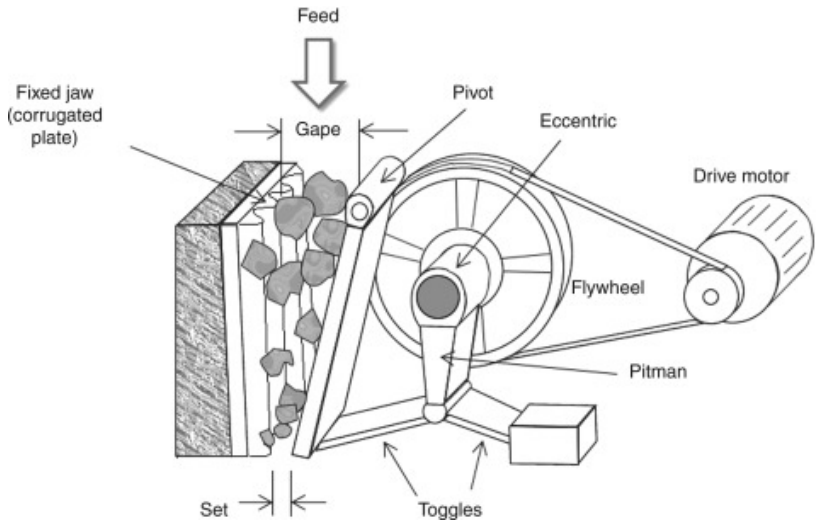

Figure 2.2: Crushing process in a crusher (A. Gupta & Yan, 2006)

A jaw crusher is defined by the width and gape i.e. $gape \times width$. In jaw crusher design, once the size of the gape is defined, the rest of the dimensions can be calculated. The size of the gape is determined from the size of the largest feed particle. These dimensions vary as manufacturers have their own catalogues and specifications for the jaw crushers (A. Gupta & Yan, 2006).

Feed size	= 0.8 -0.9 × gape
Jaw crusher width	= >1.3 - 3.0< × gape
Throw	= 0.0505 (gape) $^{0.85}$

In addition, there are variables of the feed material that are of interest during machine design. These are:

- Size of feed material

- Particle size that can fall through the chamber without being crushed at any time
- Particle size that can be nipped
- Particle size that can fall through the crushing chamber when jaws are at their widest positions.

2.2.1 Fracture Process During Comminution

Jaw crushers are compression machines which generate powerful crushing forces. For a particle to fracture, the crushing force must be greater than the fracture strength of the particle (Donovan, 2003). The rocks are usually fed into the crusher when the jaws are furthest apart. During the compression stroke, the feed material is crushed into smaller sizes and slide down the cavity as shown in Figure 2.3. This process continues until the rocks pass through the set as product.

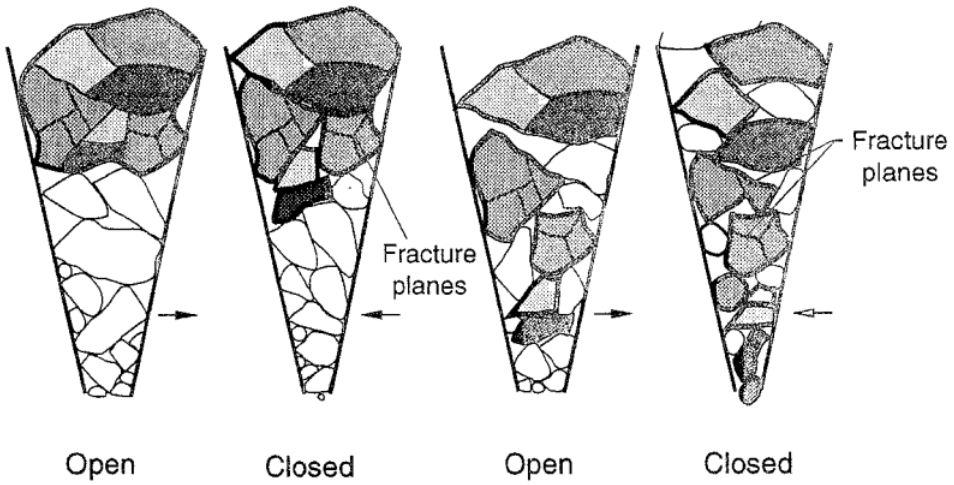

Figure 2.3: Fracture process in jaw crusher chambers (Donovan, 2003)

The characteristics of a jaw crusher with respect to design are summarised as in Table 2.1. The operator decides the size of the set during operation. The Open Side Set (OSS) is the maximum opening between the jaws while the Closed Side Set (CSS)

is the minimum opening between the jaws at discharge. The gape is the distance between the jaws at the feed opening. The throw is the stroke of the swing jaw and is defined as the difference between the OSS and CSS. If the crusher operational settings fall outside the boundaries shown in Table 2.1, the overall efficiency of the machine will decrease.

Table 2.1: Operational Parameters of a Jaw Crusher (A. Gupta & Yan, 2006)

Parameter	**Range**
Reduction Ratio, R	1:4 to 1:7
Frequency of stroke, v	100 to 300 rpm
Throw, L_T	10 to 70 mm

2.2.2 Jaw Crusher Capacity

Jaw crusher capacity can be defined as the volume or mass of crushed material per unit time. The capacity is a function of:

i. Design parameters such as width of the crushing chamber

ii. OSS and CSS (These control the reduction ratio)

iii. The type of feed method i.e. continuous feeding, intermittent feeding, manual feeding, etc.

iv. Operating characteristics such as the number of strokes per minute, stroke length (Throw)

The jaw crusher capacity is a function of eight parameters as shown:

$$Q = f(\mathrm{W}, L, L_T, n, \theta, K, L_{MAX}, L_{MIN}), \tag{2.1}$$

where,

Q = Jaw crusher capacity,

W = Jaw crusher width,

L = Height of the jaw crusher,

n = Frequency of strokes per minute (rpm),

θ = Jaw angle,

K = constant related to machine parameters,

L_{MAX} = Open set (maximum opening of the set),

L_{MIN} = Closed set (minimum opening of the set).

The capacity of jaw crushers is determined by the rate at which the rocks move down the crushing chamber. This process is a succession of jaw angles that reduce the size of the feed material until they are small enough to pass through the set. This implies that the capacity of the jaw crusher is dependent on the time taken for a particle to be crushed and dropped through each jaw angle succession until it is discharged at the bottom. Therefore, the frequency of opening and closing of the jaws are critical in jaw crusher capacity (A. Gupta & Yan, 2006).

Several researchers have tried to establish the mathematical models for determining the jaw crusher capacity. However, getting a model that takes into account all the variables affecting jaw crusher capacity is very difficult (Legendre & Zevenhoven, 2014). Manufacturers have settled on the Rose and English (A. Gupta & Yan, 2006) model in the design of jaw crusher characteristics. In this model, the maximum jaw crusher capacity Q_M is given by:

$$Q_M = 2820\ L_T^{0.5}\ \mathrm{W}\ (2L_{MIN} + L_T)\left(\frac{R}{R-1}\right)^{0.5} \rho_s\ f(P_k)\ f(\beta)\ S_c\ [\mathrm{t/h}], \tag{2.2}$$

where

R = Reduction ratio

ρ_s = Ore density in $\mathrm{t/m^3}$

P_K= Size distribution function or packing characteristics

β = The ratio of set to mean size of feed material

S_c = Parameter related to rock surface characteristics

The packing characteristics, P_K is the ratio of the difference of the maximum (d_{MAX}) and minimum (d_{MIN}) to the mean size of feed material (d_{MEAN}):

$$P_K = \left(\frac{d_{MAX} - d_{MIN}}{d_{MEAN}}\right). \tag{2.3}$$

P_K, and β can be related to jaw crusher capacity by the functions $f(P_k)$ and $f(\beta)$ respectively. This relationship is as shown in Figure 2.4. For all practical purposes, $f(\beta)$ is equal to 1 because the closed set must always be less than the feed size.

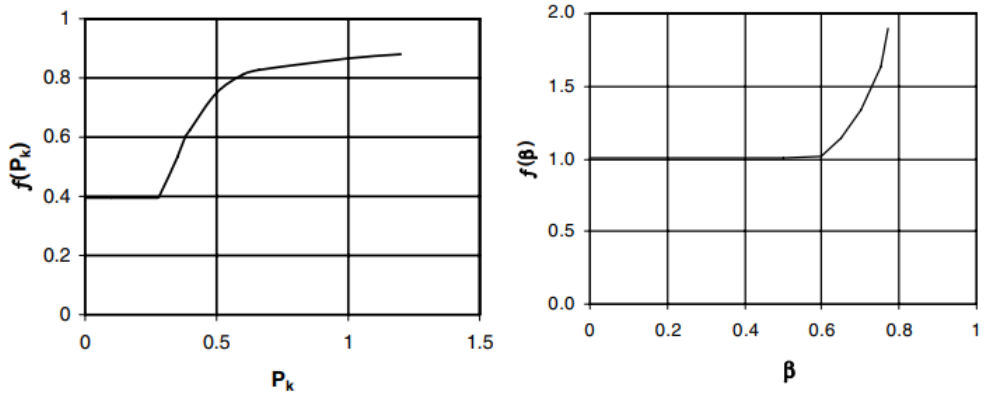

Figure 2.4: Relationship between β, $f(\beta)$, P_K and $f(P_k)$ (A. Gupta & Yan, 2006)

It has also been found that beyond a certain operating frequency, the productivity of the crusher decreases (A. Gupta & Yan, 2006). This frequency is the critical crusher frequency and is given as:

$$v_c = 47 \, \frac{1}{(L_T)^{0.5}} \left(\frac{R-1}{R} \right)^{0.5} \quad \text{[cycles/min]}. \tag{2.4}$$

Therefore, for actual crusher speeds, v, the actual capacity of a jaw crusher, Q_A, is given by;

$$\begin{aligned} Q_A &= Q_M \, \frac{v}{v_c} \quad \text{for} \quad v < v_c \text{ and} \\ Q_A &= Q_M \, \frac{v_c}{v} \quad \text{for} \quad v > v_c. \end{aligned} \tag{2.5}$$

If $v = v_c$, then Q_A will be equal to Q_M and in this case, the maximum capacity for production is theoretically achieved.

2.2.3 Jaw Crusher Power

Expressions for approximating the power consumption of a jaw crusher have been developed by various authors (A. Gupta & Yan, 2006; Legendre & Zevenhoven, 2014). Basically, there are four laws of comminution energy.

1. **Rittinger's Law**: Rittinger assumes that the energy consumed is directly proportional to the new surfaces created. Therefore, specific surface area is inversely proportional to the particle size. The specific comminution energy E/m is given by (Kanda & Kotake, 2007):

$$\frac{E}{m} = C_R(S_P - S_F), \tag{2.6}$$

where, C_R is a constant that depends on the characteristics of the material. S_P, S_F and m are specific surface areas of the product and feed, and mass respectively.

2. **Kick's Law**: Kick law states that the energy required for comminution is related only to the ratio between feed size and product size (Kanda & Kotake, 2007).

$$\frac{E}{m} = C_K \ln\left(\frac{x_f}{x_p}\right), \tag{2.7}$$

where x_p and x_f are the particle sizes of product and feed respectively while C_k is a constant. Equation 2.7 can be derived by assuming that the strength is independent on particle size and the energy for size reduction is proportional to the volume and size reduction is constant at each stage of comminution. This is in contradiction to Griffith's weakest link theory which mentions that as particles get smaller, they become more resistant to fracture.

3. **Bond's Law**: Bond approach has always been used in predicting the energy consumption during the size-reduction process. Bond Work Index coefficients cover almost the entire range of particles that are to be processed using comminution machinery (Schroe, 2016). Bond suggests that any comminution process can be considered to be an intermediate stage in the breakdown of a particle of infinite size to an infinite number of particles of zero size. Bond's theory states that the total work useful in breakage is inversely proportional to the square root of the size of the product and feed particles (Kanda & Kotake, 2007):

$$W = W_i\left(\frac{10}{\sqrt{P_{80}}} - \frac{10}{\sqrt{F_{80}}}\right), \tag{2.8}$$

where, P_{80} and F_{80} are the particle sizes in microns at which 80% of the corresponding product and feed passes through the sieve. W_i is the Bond's work index and is crucial in designing the comminution processes.

4. **Holmes' Law**: Holmes' law is a modification of Bond's law in which the square root is replaced by an exponent r as shown below (Kanda & Kotake, 2007):

$$W = W_i\left(\frac{10}{P_{80}^r} - \frac{10}{F_{80}^r}\right), \tag{2.9}$$

The values of r are determined experimentally for different materials (Kanda & Kotake, 2007).

The most popular method for determining the power consumption or draw of a comminution machine is the Bond's method. However, the laws of comminution have a few weaknesses; they are not suitable for evaluation of primary crushing equipment processing large particle sizes, they only fit experimental data over a limited range of variables and suitable for only certain cases and Bond's work results in a conservative overdesign of the crushing plant. To counter these weaknesses, Single Particle Breakage analysis is currently being adopted to relate fracture energy and product size distribution to a materials property. During the fracture of a single spherical particle, the elastic strain energy, Y (J), input up to the instant of fracture is given by (Kanda & Kotake, 2007):

$$Y = 0.832\left(\frac{1-\nu^2}{E}\right)^{\frac{2}{3}}(D)^{-\frac{1}{3}}(P)^{\frac{5}{3}}, \tag{2.10}$$

Where, E (Pa) is Young's Modulus, ν (-), Poisson's ratio, D (m) the diameter of the sphere and P (N) the fracture load.

In addition, the Rose and English model has been used to determine the power consumption of a jaw crusher. This model involves the use of Bond's work index in power calculation. The actual power consumption of a jaw crusher is given by (A. Gupta & Yan, 2006):

$$P_A = 0.01195\, W_i\, Q_A \left[\frac{\sqrt{G} - 1.054\sqrt{(L_{MIN}+L_T)}}{\sqrt{G}\sqrt{(L_{MIN}+L_T)}}\right] \text{[kWh/t]}, \tag{2.11}$$

where,

P_A = Actual power consumption,

W_i = Bond's work index,

G = Jaw crusher gape.

2.3 Fracture Mechanics

Rock properties affect the energy consumption and performance of a jaw crusher. Fracture properties such as particle strength, breakage fragment size distribution and specific breakage energy of a material have been known to affect the power consumption of size-reduction machines. Fracture toughness can be defined as an intrinsic material property which depicts the material's resistance to crack propagation (Donovan, 2003).

The energy required for comminution can be determined by the surface area created. As the particle sizes decrease, the number of new surface areas increase. Therefore, measuring the surface area before and after size-reduction process can be a good indicator of the amount of energy used in comminution. During fracture, energy is consumed in the following ways:

- Creation of new surfaces such as internal cracks.
- Kinetic energy and rotation energy carried by flying and rotating fragments respectively.
- Through heat and plastic deformation at crack tips.
- Energy consumption in releasing sound and electromagnetic radiation.
- Other processes such as friction between mineral grains.

2.3.1 Griffith's Theory

Griffith theory proposed that inherent cracks within a brittle material are main cause of failure. In Figure 2.5, the stress σ_A is the tensile strength. If the material

completely fractures as a result of the applied stress, then σ_A is the fracture strength and the corresponding stress at C is the molecule strength or theoretical strength of the material. Fracture in a rock sample with inherent cracks usually starts at point C. Therefore, the stresses at point C determine whether or not a crack will initiate.

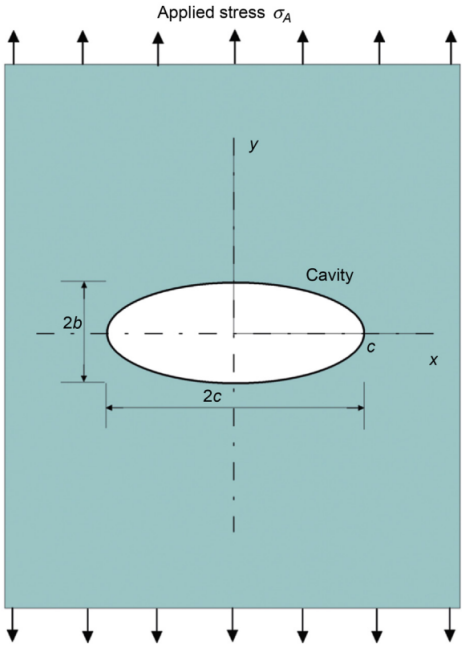

Figure 2.5: An elliptical cavity inside a plate (Zhang, 2016)

How a particle breaks during comminution is a difficult process to understand. For instance, sub-processes which take place before material failure are dependent on the type of comminution machine used and also pre-existing flaws within the material. The mechanism of failure affect the product size distribution. In addition, pre-existing cracks act as stress concentrators hence facilitating crack propagation.

In critical conditions, i.e. when the material failure occurs, $\sigma_A = \sigma_F$ and $c = c_0$ and thus (Zhang, 2016);

$$\sigma_F = \sqrt{\frac{2E\gamma}{\pi c_0}}. \tag{2.12}$$

Equation 2.12 is the Griffith strength relation where σ_F is the fracture stress, E is Young's modulus and γ is the surface fracture energy per unit area. Equation 2.12

shows that fracture stress depends on the crack length, c, and hence fracture stress is not a material property. Modifying the equation (Zhang, 2016);

$$\sigma_F \; c_o^{\frac{1}{2}} = \sqrt{\frac{2E\gamma}{\pi}}. \tag{2.13}$$

In Equation 2.13, the right side has constants E and γ which are material properties and the left side represents fracture toughness which is a material property. Griffith strength relationship shows that materials with shorter crack lengths require higher applied stresses to fracture than materials with longer cracks. This can be related to Weibull's weakest link theory which states that *the strength of a particle is dependent upon its most critical flaw.* As the particle size decreases, the probability of a critical flaw reduces. This implies that bigger particles have a higher probability of failure than smaller ones.

The bounding surfaces in a solid, just as in liquids, posses surface tension which confirms the presence of a corresponding amount of surface energy. Therefore, for a crack to be formed, the magnitude of applied energy must be proportional to the area of the new surfaces created (Zhang, 2016). Measuring the surface area before and after size reduction could be an indicator of how much energy is used in comminution (Legendre & Zevenhoven, 2014). Therefore, the new surface area created will be used in this research to obtain the energy efficiency of the single toggle jaw crusher.

2.3.2 Relationship between Fracture Toughness and Energy

Fracture mechanics deals with the study of individual crack formation and propagation in solid particles as a result of applied stress. Fracture toughness is the most fundamental parameter in fracture mechanics as it describes the resistance to crack extension. Therefore, sufficient strain energy must be released to overcome the surface energy (Zhang, 2016).

Based on Griffith theory;

$$G = G_C, \tag{2.14}$$

where, G is the strain energy release rate (or crack propagation force) and G_C is the fracture toughness or critical strain energy release rate.If G is equal to G_C, crack extension takes place. The strain energy release rate G can also be related to the stress intensity factor K. For Mode I crack,

$$G_I = \frac{K_I^2}{E^*}, \tag{2.15}$$

where, G_I is the strain energy release rate for Mode I and K_I is the stress intensity factor for Mode I nature of fracture. E^* is the effective Young's modulus (Zhang, 2016);

$$\begin{aligned} E^* &= E \quad \text{for plane stress} \quad \text{and} \\ E^* &= \frac{E}{1-\nu^2} \quad \text{for plain strain,} \end{aligned} \tag{2.16}$$

and ν is the material's Poisson's ratio.

In engineering, rock failure often originates from one or multiple cracks in micro or macro scale. For instance, during rock blasting, rocks are shattered into fragments as a result of crack propagation. Therefore, to solve a fracture problem, one has to understand fracture mechanics theory. To know whether a crack will propagate, the energy release rate or stress intensity factor should be determined. It is also important to note that the stresses at or near crack tips vary as the cracks extend hence rock failure is a complex dynamic problem (Zhang, 2016).

2.3.3 Relationship between Fracture Toughness and Rock Strength

Tensile strength σ_t, compressive strength σ_c and shear strength of rocks σ_s are related to each other. Laboratory tests have shown that tensile strength is the minimum

while compressive strength is the maximum (Zhang, 2016). Shear strength usually falls in between. This relation can be mathematically expressed as;

$$\sigma_c = a\ \sigma_t = b\ \sigma_s, \tag{2.17}$$

where a and b are constants. Under uniaxial tensile and compressive strength testing, b is usually smaller than a and $8 \leq a \leq 15$. Equation 2.17 shows that compressive strength has higher values than shear and tensile strengths. This implies that rocks are easily fractured when subjected to tensile or shear load. Compressive tests in an SEM (scanning electronic microscope) of small rocks was conducted by Zhao (Zhao, 2017) and it was observed that crack propagation ran along grain boundaries. This implied that the fracture was tensile in nature (Sprunt, 2000). Tapponier and Brace (Tapponnier & Bracet, 1976) observed that most cracks under compressive loading were straight, long, narrow with sharp ends implying that they were tensile in nature.

Fracture toughness is a material property but strength is not. However, fracture toughness is harder and costly to measure than strength (Zhang, 2016) . Therefore, experiments have been conducted to establish an empirical relation between Mode I fracture toughness and tensile strength of rocks as shown in Equation 2.18 (Zhang, 2016);

$$K_{IC} = \frac{1}{6.88}\ \sigma_t, \tag{2.18}$$

In rock engineering, crack initiation and propagation are very critical. Hoek and Martin (Hoek & Martin, 2014) conducted a review on fracture initiation and propagation in intact rock . Tensile fracture was found to increase as loading in confined pressure increased. The tensile fracture seemed to initiate at 40% - 60% of the uniaxial compressive strength. Griffith theory of brittle failure provided a simplified model based on the assumption that all fractures initiate from the tips of existing flaws. Even though fracture initiation in tensile loading is more complex

to model, DEM has shown that a force-chain crack model is a good alternative for tensile fracture modelling.

Khanal (Khanal, 2005) conducted a detailed investigation of how spherical particles fracture under impact and crushing stressing. Concrete was subjected to central and oblique impacts using single and double plate moving walls . Fracture and fragmentation behaviour of heterogeneous solids was studied. The author also analysed the size distributions of the fragments arising from comminution. Three different crack analysis techniques were investigated; discrete element, finite element and experimental methods. It was observed that finite element method was only limited to some extent in analysing crack propagation in that the actual fracture could not be modelled. Therefore, discrete element method was adopted. It was also concluded that particle shape influenced the size distributions and velocity did not always generate finer particles. However, the spherical particles used in the simulations were not bonded hence crushing or grinding aspect was not fully captured.

Olaleye (Olaleye, 2010) investigated the influence of some rock strength properties on jaw crusher performance in a granite quarry. The main objective of the study was to determine how rock strength affects the grain size distribution and also the crushing time of the jaw crusher. Four rock samples were used; granite, dolomite, marble and limestone. Point load and unconfined compressive strength tests were conducted on each sample. Granite was recorded to have the highest unconfined compressive strength and longest crushing time. It was concluded that rock strength plays a major role in crushing time of rocks. However, the efficiency and performance of the jaw crusher was not conducted.

Rusell et al. (Russell, Muir Wood, & Kikumoto, 2009) subjected four idealised assemblies of equally sized spherical particles to a range of macroscopic compressive principal stresses . The contact forces and stress fields within individual particles

were studied. Individual particles located within the assembly was subjected to discrete forces at contact points with adjacent particles and hence the corresponding stress state within each particle will be non-uniform. It was concluded that crushing of individual particles within a granular assembly subjected to macroscopic stresses is a function of the force with the highest magnitude acting on that particle cluster. Particle geometry was found to indirectly influence crushing except in particles which were densely packed. Lesser contact forces were found not to directly affect the crushing process. However, use of equally sized spheres failed to bring out the heterogeneity property found in rocks.

2.4 Comminution Energy Efficiency

Comminution is an energy intensive process. However, based on the energy required to create new fracture surface relative to the mechanical energy input, the energy efficiency of the size-reduction process is very low. Researchers have proposed use of new surface area created as a method of assessing the energy efficiency of a comminution machine (Tromans & Meech, 2002). Single particle breakage techniques have been adopted in the past to determine comminution energy efficiency (Tromans, 2008).

2.4.1 Theoretical Energy Efficiency

The theoretical maximum limiting energy efficiency, η_{limit}, is examined with respect to brittle fracture of rocks under uniaxial tensile loading which is followed by compressive loading (Tromans & Meech, 2002). Here, the fracture is initiated at pre-existing flaws(crack) as shown in Figure 2.6. The maximum energy limiting efficiency is based on the energy required to create new fracture surface.

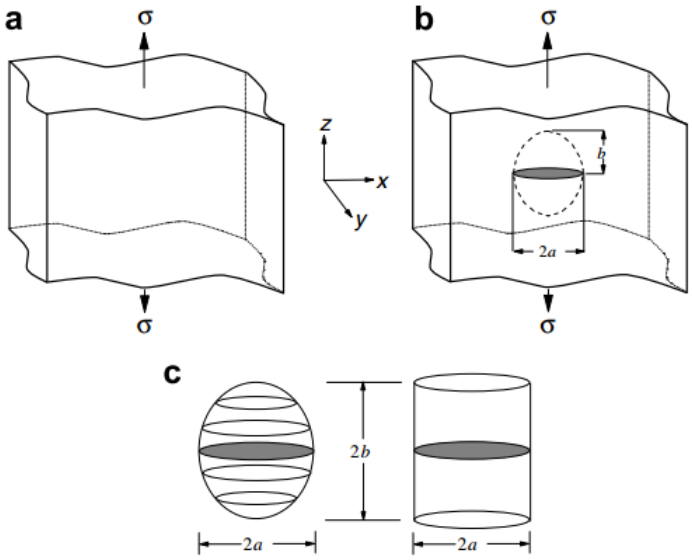

Figure 2.6: Uniaxially stressed body (Tromans, 2008)

An isotropic solid body shown in Figure 2.6a is subjected to tensile stress σ parallel to the z-axis. In Figure 2.6b, a penny-shaped crack of radius a is introduced and lies in the $x - y$ plane. At the free surfaces of the crack, tensile stresses will be zero and hence a region of stress relaxation on both sides of the disc will exist. Troman approximated that all sections parallel to the $x-y$ plane are circles and those parallel to the $x - z$ plane are ellipses for the purpose of analysis. After analysis, it was concluded that the maximum limiting energy efficiency of fracture under uniaxial tensile loading cannot be greater than 66% (Tromans & Meech, 2002). The 66% was obtained from the ratio of the strain energy caused by the growth of the ellipse to that of the strain energy available for crack growth in the the cylinder as shown in Figure 2.6 c. In Figure 2.7, a particle with an approximate diameter D is subjected to compressive load P just as in comminution process.

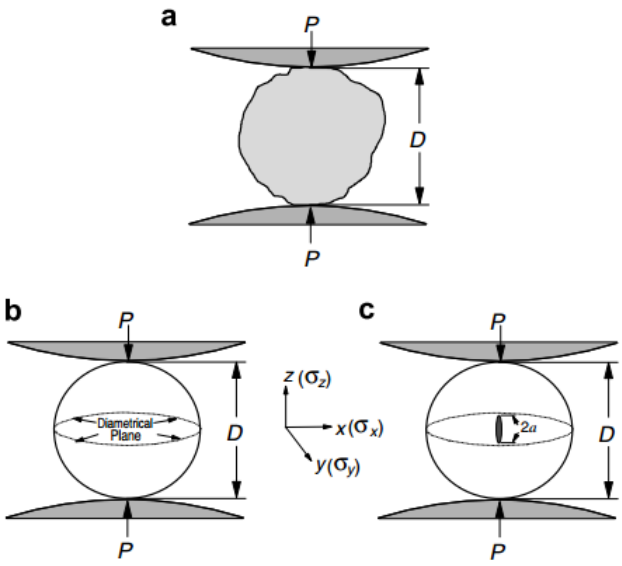

Figure 2.7: Particle approximated to a sphere of diameter *D* under compressive load *P* (Tromans, 2008)

In Figure 2.7b, the particle is approximated to a sphere of diameter D which is oriented with respect to the Cartesian co-ordinate system. The compressive load acts along the $z-axis$ passing through the centre of the sphere normal to the $x-y$ plane. The maximum tensile force due to the applied load generates a normal stress σ_z and radial stresses σ_x and σ_y. The radial stresses are equal for all rotations around the $z-axis$. Hu et al. (G. Hu, Otaki, & Lin, 2001) performed an analysis on the values of the three stresses, σ_x, σ_y and σ_z, present at the centre of the sphere and concluded:

$$\sigma_x = \sigma_y = \frac{P}{\pi D^2}\left(\frac{6(1-2\nu)}{2+\sqrt{2}}\right), \tag{2.19}$$

$$\sigma_z = -\frac{P}{\pi D^2}\left(12 - \frac{3}{\sqrt{2}}\right). \tag{2.20}$$

Due to the triaxial stress state at the centre of the sphere, the strain energy per unit

volume ($(S_E)_3$) is given by the Equation (Tromans, 2008):

$$(S_E)_3 = \left(\frac{1}{2E}\right)[(\sigma_x^2 + \sigma_y^2 + \sigma_z^2) - 2\nu(\sigma_x\sigma_y + \sigma_x\sigma_z + \sigma_y\sigma_z)]. \tag{2.21}$$

In Figure 2.7c, a small thin disc shaped crack with a radius a is introduced. The plane of the disc is normal to the $x - axis$ and lies in the $y - z$ plane. There will be an area of stress relaxation around the disc hence σ_x will be relaxed to zero leading to a biaxial state at the centre of the sphere. Therefore, equating $\sigma_x = 0$ in Equation 2.21, the new strain energy per unit volume due to the biaxial stress is:

$$(S_E)_2 = \left(\frac{1}{2E}\right)[(\sigma_y^2 + \sigma_z^2) - 2\nu(\sigma_y\sigma_z)]. \tag{2.22}$$

To obtain the strain energy released per unit volume due to the crack, Equation 2.22 must be subtracted from Equation 2.21:

$$(S_E)_3 - (S_E)_2 = \left(\frac{1}{2E}\right)[(\sigma_x^2 - 2\nu(\sigma_x\sigma_y + \sigma_x\sigma_z)]. \tag{2.23}$$

Dividing Equation 2.23 by Equation 2.21 and multiplying by 66% will give the maximum limiting energy efficiency of comminution, η_{Limit} (the ratio of the volumes of the ellipsoid defect to the accommodating cylinder) (Tromans, 2008):

$$\eta_{Limit} = \left[\frac{\sigma_x^2 - 2\nu(\sigma_x\sigma_y + \sigma_x\sigma_z)}{(\sigma_x^2 + \sigma_y^2 + \sigma_z^2) - 2\nu(\sigma_x\sigma_y + \sigma_x\sigma_z + \sigma_y\sigma_z)}\right] \times 66\%. \tag{2.24}$$

Equation 2.24 gives the maximum limiting energy efficiency of comminution, η_{Limit}. However, η_{Limit} is only a function of Poisson's ration, ν, and hence it is not affected by the applied load or particle size (Legendre & Zevenhoven, 2014; Tromans, 2008). In essence, η_{Limit} is a material property hence it cannot be used independently to obtain jaw crusher energy efficiency.

2.4.2 Actual Energy Efficiency

As mentioned earlier, the size reduction process leads to a reduction in particle size which in turn increases the new surface areas created. Therefore, the energy used in comminution can be determined by measurement of the surface area before and after size reduction process.

Efficiency of a comminution machine can be defined as the ratio of the measure of output from a size reduction machine to the amount of supplied energy. However, this term has been surrounded with controversial arguments; for instance, extremely low energy efficiencies of 1-3% are almost meaningless (Fuerstenau & Abouzeid, 2002). In real comminution systems, most of the strain energy required to initiate crack propagation is lost in form of heat, noise and mechanical vibrations. More evidence has shown that the efficiency of a comminution system is dependent on the comminution system. Surface area and surface energy have been used widely for the assessment of comminution efficiency (Fuerstenau & Abouzeid, 2002).

Efficiency can also be defined as the ratio of an ideal system behaviour to the real system or process behaviour. For comminution processes, the increase in specific surface energy (ΔS_{En}) has been accepted as a comparison point since it represents the quantification of the new surface area created during fracture. Tromans and Meech (Tromans & Meech, 2002) related the new surface area as a result of crack propagation to the respective particle diameter. An increase in surface energy per unit mass as a result of particle fracture is, therefore, approximated by:

$$\Delta S_{En} = \frac{\gamma A_{Created}}{M} \approx \frac{6F_r\gamma}{\rho}\left(\frac{1}{(D_f)_s} - \frac{1}{(D_i)_s}\right) \text{ [J/kg]}, \tag{2.25}$$

where,

γ = fracture surface energy [J/m^2],

$A_{Created}$ = New surface area created [m^2],

M = Total particle mass [kg],

ρ = material density [kg/m^3],

$(D_f)_s$ and $(D_i)_s$ = Final and initial surface mean diameters [m],

F_r = Dimensionless surface roughness factor that corrects for non-sphericity,

If the specific energy is the ideal energy requirement of the size reduction process, the classical energy efficiency, $\eta_{Classical}$, is the ratio between ΔS_{En} and the actual energy requirements for the comminution process, $E_{Equipment}$. In reality, the energy requirements for a size-reduction machine are higher than the ideal energy requirements as shown in Equation 2.25. The total energy efficiency of the system is the ratio of the classical efficiency to the maximum limiting theoretical energy efficiency;

$$\eta_{EnergyTotal} = \frac{\eta_{Classical}}{\eta_{Limit}} = \frac{\Delta S_{En}}{\eta_{Limit}\ E_{Equipment}}. \tag{2.26}$$

The power consumption of the swing jaw is obtained from the compressive force, F, and velocity, V, as shown:

$$P = F.V \text{ [W]}. \tag{2.27}$$

Integrating Equation 2.27 with respect to time, the energy used per time step during the simulation will be obtained, i.e.

$$E = \int P dt \text{ [J]}. \tag{2.28}$$

Fracture surface energy has been linked to the energy efficiency of comminution machines by various authors (Fuerstenau & Abouzeid, 2002; Legendre & Zevenhoven, 2014; Tromans, 2008). However, the cross-sectional area have been used in determining the work of fracture rather than the actual area. This has resulted

in huge estimates. Smith et al. (Smith, Mecholsky, & Freiman, 2009) developed an equation for actual fracture area, A_F, of soda-lime-silica glass using chevron-notch tests. It was concluded that use of A_F resulted in less values of work of fracture than when using cross-sectional areas. The calculations obtained only provided an estimate of the minimum energy required to break bonds during fracture.

Assessing the energy efficiency of a jaw crusher was conducted by Legendre and Zevenhoven (Legendre & Zevenhoven, 2014). DEM was used in rock modelling and simulation of the crushing process. The jaw crusher throw and toggle speed frequency were varied according to Table 2.1. However, the reduction ratio was varied from 1:4 to 1:9. A GA code was also implemented so as to minimize the energy consumption of the jaw crusher. The rock model used in the simulation was spherical in nature and its mechanical properties were that of limestone. The jaw crusher efficiency was analysed from the new fracture area created. However, the modelled rock seemed to collapse into individual DEM particles. This was probably due to the weak bond calibration in DEM simulation software. To approximate the experimental energy consumption of the jaw crusher, Bond work index theory was employed. The maximum theoretical energy efficiency obtained was 20.6% via simulations which were validated using experiments. Even though energy assessment was done, maximisation of energy efficiency was not done and parameters which have an impact on efficiency were not identified.

Bharule (Suresh, 2009) and Deepak (Deepak, 2010) conducted an analysis of the swing jaw plate of a jaw crusher. The stiffness of the swing jaw plate was varied with the aim of reducing the plate weight while also increasing the overall stiffness. Finite element analysis of the swing jaw plate was conducted using eight-node brick elements. It was concluded that stiffened jaw crusher plate lead to energy savings of about 25%. The feed material was also arranged inside the crushing chamber and this depicted the maximum capacity which can be crushed during one cycle. Ramkrushna (More & Raisoni, 2014) conducted a design analysis of the swing jaw

plates by introduction of stiffeners. FEA was used to determine the optimal number of stiffeners in the swing jaw and the final model led to about 35% energy savings. However, the particles were not crushed as DEM was not applied.

Radziszewski (Radziszewski, 2013) conducted a research with the aim of developing an energy recovery system for comminution machines. Four issues addressed in the paper were; potential energy recovery, heat generated in comminution, possible means of energy recovery in comminution and possible fields where the recovery systems could be applied. Insulation and sealing of the grinding circuit was recommended as it increased the circuit efficiency by 10%. In the research, only SAG and ball mills were considered. Even though some of the energy loss was minimized, the energy efficiency of comminution process was still very low hence more work on optimisation have to be done.

2.5 Genetic Algorithms and Design of Experiment

During the size-reduction process in a jaw crusher, three critical parameters determine the power consumption and also the energy efficiency i.e. the *throw*, the *toggle speed* and the *reduction ratio*. However, getting a relationship that takes into account all the relevant variables during comminution is hard (Tromans, 2008).

Genetic algorithms (GAs) are numerical optimisation algorithms which are inspired by both natural selection and natural genetics. A typical algorithm uses three operators, selection, crossover and mutation (chosen in part by analogy with the natural world) to direct the population (over a series of time steps or generations) towards convergence at the global optimum (Coley, 1999). There are many types of Genetic Algorithms which come with different representations. The two most important GAs are the Simple Genetic Algorithm (SGA) and the Differential

Evolution (DE) methods. It has been shown that a SGA code has a better potential of solving power consumption than a DE code (Legendre & Zevenhoven, 2014).

Design of Experiment (DOE) can be defined as a methodology for systematically applying statistics to experiments. The most common methods used in DOE are Full factorial design and Taguchi method. The Taguchi method has been widely used in many engineering analyses. DOE provides a predictive knowledge of multi-variable processes with few trials hence reduces the time required for experimental or simulation investigations (Rafidah et al., 2014).

Rafidah (Rafidah et al., 2014) conducted a comparison between Taguchi method and Full factorial design technique on surface roughness measurement . Full factorial method is suitable for two-level design experiments or simulations. On the other hand, Taguchi method is suitable in identification of design factors which affect critical process characteristics. In Full Factorial design, the total number of runs are given by (Rafidah et al., 2014):

$$\text{Runs} = G^t, \tag{2.29}$$

where, G is the number of limits and t is the number of variables within the simulations. Rafidah used MINITAB software to compare the two techniques and concluded that both techniques are good for DOE procedures. However, the full factorial design had less mean square error and provided an efficient methodology for optimisation of process parameters hence was superior to Taguchi method.

According to Lee (LEE, 2012), better crushing machines can be obtained by optimising a given crushing process theoretically before actual machine design. Complex breakage behaviours of gneiss, diabase, marble and quartzite were mathematically modelled and experimentally studied. A GA code was implemented to theoretically optimise the compressive crushing of a cone crusher. The objective function and type of application seemed to affect the theoretical optimisation of a cone crusher. Theoretical efficiencies of 30%-40% were attained. It was recommended

that DEM should be used in investigating how different machine parameters, such as stroke, affect performance of comminution machines. DEM simulations would also couple the dynamics of rocks within the crushing chamber as opposed to continuum approach such as Finite Element Method (FEM).

Numbi et al. (Numbi, Zhang, & Xia, 2014) developed two optimal control models for energy management in a comminution process on jaw crushers. The first control model was based on the feeding rate and CSS of the jaw crusher. The second model was based on optimal switching control in which the machines were switched depending on the linear velocity of the apron feeder, mass flow rate of the ore and mass of the ore. The optimal switching control method led to higher energy savings but at the cost of switching the machines. However, in the research, the start-up and shut down energy of the jaw crusher are neglected. Furthermore, addition of an additional switching control model would lead to a design which is more costly to implement.

Khaled developed an ANFIS model with the aim of predicting the power consumption of a jaw crusher (Abuhasel, 2019). The model was developed using MATLAB software and thirty two specific energy consumption values were measured at different crushing conditions. Eight more data sets were then used to determine the accuracy of the generated model. However, Khaled used reduction ratios of 1.5 and 2.97 which do not agree with the values adopted for jaw crusher design (A. Gupta & Yan, 2006; Legendre & Zevenhoven, 2014). In addition, the toggle speed and throw were neglected during the predictions.

2.6 Discrete Element Method

Discrete Element Method was first developed by Cundal and Strack (Cundall & Strack, 1979) as a numerical model which describes the mechanical behaviour of assemblies of spheres or discs. A granular material is composed of distinct particles

which act independently from each other and interact only at contact points. The discrete nature of such materials results in complex behaviour under loading and unloading conditions.

Discrete Element Method (DEM) is suitable for simulation of discrete matter, such as granular materials or powders, in a series of events known as time steps. In DEM, individual particles are tracked as they interact with other particles within the system boundary (Legendre & Zevenhoven, 2014; Quist, 2012). DEM is a simulation tool which can replicate the motion and interaction of rigid independent particles using Newton's second law of motion and contact models. By applying the Newton's second law of motion per time-step, simulation of particle flow in machine domains is now possible (EDEM, 2012). In DEM, external force fields can now be added into the simulation in order to simulate the influence of electrostatics and air drag. The steps involved in DEM simulation are as shown in Figure 2.8.

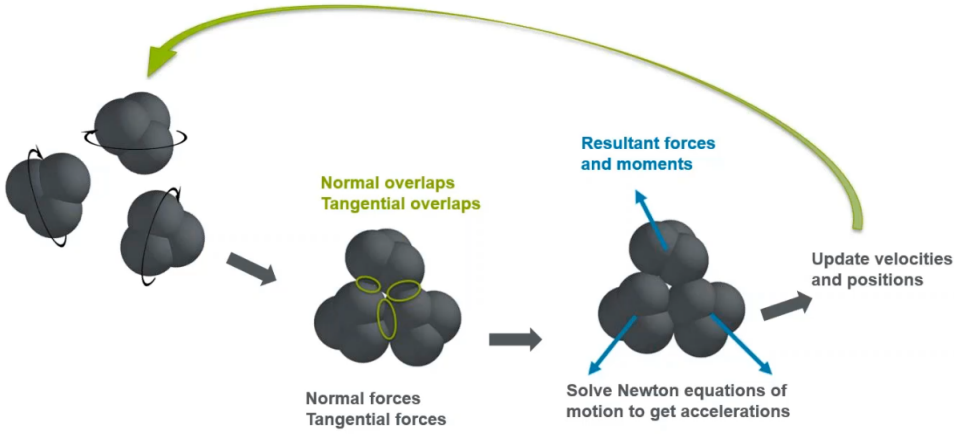

Figure 2.8: Steps of DEM simulation (EDEM, 2012)

In DEM, the interaction between individual particles is treated as a linear spring dashpot contact model. This is suitable for determining at what point the particles will break as a result of the applied force. In Figure 2.9, the particles allowed to overlap and denoted by Δx. The normal v_n and tangential v_t relative velocities are also used in determination of the collision forces. The normal force is given by (Zhao,

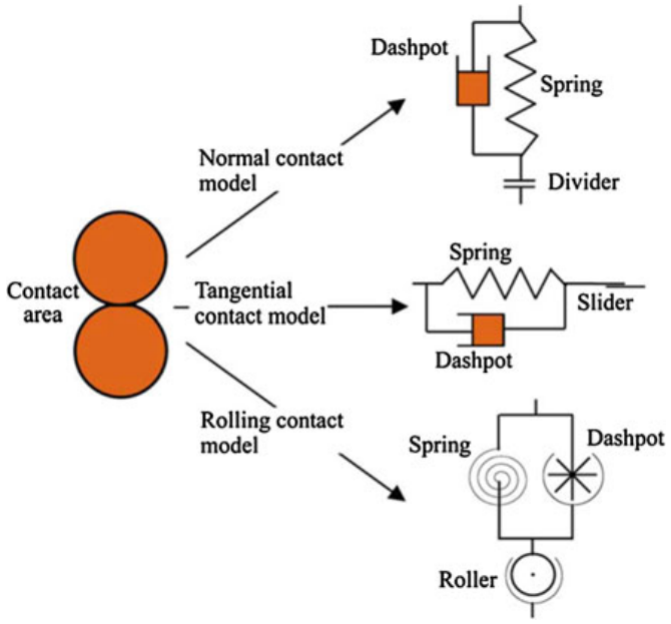

Figure 2.9: Contact model between two spheres (Zhao, 2017)

2017):

$$F_n = -k_n \Delta x + C_n v_n, \tag{2.30}$$

where,

$$C_n = 2\lambda\sqrt{m_{ij} k_n}, \tag{2.31}$$

$$\lambda = \frac{-ln(\epsilon)}{\sqrt{\pi^2 + ln^2(\epsilon)}}, \tag{2.32}$$

$$m_{ij} = \frac{m_i m_j}{m_i + m_j}, \tag{2.33}$$

and

C_n= Damping coefficient of normal force in Ns/m,

k_n= Normal stiffness in N/m,

ϵ= Coefficient of restitution.

Equation 2.30 has a linear spring to provide the repulsive force and a dashpot to

dissipate a proportion of the relative motion. The term ϵ represents the coefficient of restitution which is defined as the ratio of the post-collisional to pre-collisional normal component of the relative velocity. In Equation 2.33, the term m_{ij} represents the reduced mass of particles i and j with masses m_i and m_j respectively.
The tangential force is given by (Zhao, 2017):

$$F_t = min\left\{\mu F_n \sum k_t v_t \Delta t + C_t v_t\right\}. \tag{2.34}$$

F_t and v_t are defined in the tangent plane at the contact point. The summation term in Equation 2.34 represents an incremental spring that stores energy from the relative tangential motion and corresponds to the elastic tangential deformation of the contacting surfaces. The dashpot produces dissipation of energy in the tangential direction and represents plastic deformation of the contact in the tangential direction.

In particle modelling, two methods can be used; continuum approach and discrete approach (EDEM, 2012). In continuum approach, it is assumed that the modelled particle is continuous and occupies the entire space. Therefore, behaviour of individual particles is ignored implying that the resulting equations are solved numerically and this involves Finite Element Methods. On the other hand, discrete approach handles individual particles as separate entities i.e. each particle has a unique quantity. The material is therefore considered as an assembly of particles as shown in Figure 2.10.

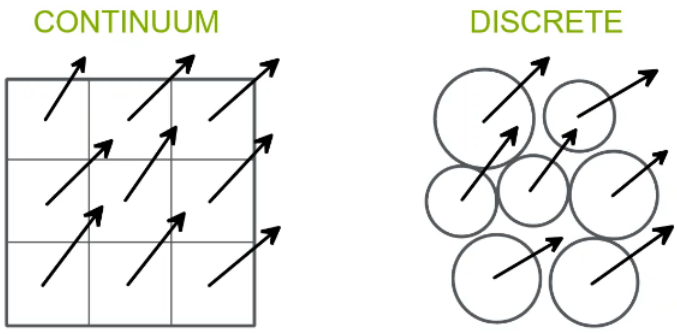

Figure 2.10: Continuum and discrete approach (DEM Solutions, 2016)

2.6.1 Types of Breakage Models used in DEM

In DEM, rock breakage modelling is dominated by two strategies; the Bonded Particle Model (BPM) and the Particle Replacement Model (PRM). In particle replacement model(PRM), the breakage phenomena is mimicked by replacement of particles i.e. if a particle is subjected to a load greater than its critical strength, it is replaced by a number of progeny particles of predetermined size. The strength of the particles and size distribution of progeny particles are gathered from experiments. PRM is ideal for simulating size-reduction processes in which impact force is dominant (Quist, 2012).

Bonded particle model (BPM) is based on 'glueing' particles together using bonds resulting in an agglomerated cluster. Breakage occurs when the applied force exceeds the critical strength of the bonds. Here, the particles are actually broken down into smaller clusters which preserve the dynamics of the 'parent' particle (Quist, 2012). In PRM the progeny particles are decoupled from the 'parent' particles hence losing initial particle dynamics. In a jaw crusher, the crushing sequence is dependent on particle flow dynamics hence BPM will be adopted in this research.

Jimenez (Jiménez-Herrera, Barrios, & Tavares, 2017) compared three models which can be used in simulation of particle breakage. BPM, PRM and Fast breakage model (FBM) were compared. Jimenez concluded that BPM is ideal for processes in which the interaction between particles and crushing equipment walls is crucial. In addition, FBM and PRM failed to fully describe the force-deformation profile while BPM emerged superior. Therefore, in this research, the BPM will be adopted for breakage analysis. In addition, DEM was found to demand massive amounts of computational power and hence particle sizes varying between 2 mm and 35 mm were recommended.

Discrete element method has been used to solve complex problems in comminution

(Weerasekara et al., 2013). The application of DEM in simulation of breakage, crushing, fracture and equipment wear has increased not only in size but also in complexity. Weerasekara et al. (Weerasekara et al., 2013) reviewed the contribution of DEM to the science of comminution. It was concluded that the major challenges in DEM is incorporation of finer particles in simulations. On the other hand, researchers can include dynamic particle breakage in DEM and this makes evaluation of crusher performance viable and hence can be used in particle flow predictions.

Schubert (Schubert, 2005) conducted a research on the breakage process using DEM in an impact crusher. Concrete was used as the research specimen. The modelling of the concrete was done by larger particles and smaller particles which represented the aggregates and hardened cement respectively . The total number of particles used per simulation varied between 400 and 6400 particles. It was concluded that 400 particles were sufficient for rough simulations while more than 1600 particles were ideal for precise simulations. The higher the number of particles, the longer the simulation time. Particle Flow Code (PFC) software was used. Here, instead of using real 3D, the author modelled 2D concrete models and linked them with a 3D vector graphic program. In doing so, the particle dynamics in the *z-axis* were only replicated hence did not achieve the desired realism. Therefore, there is need to model 3 dimensional DEM rock models for the breakage process.

Refahi et al. (Refahi, Mohandesi, & Rezai, 2010) investigated the relationship between bond crushing energy and fracture energy of rocks in a jaw crusher using numerical simulation. DEM was employed in modelling the crushing behaviour of rocks using PFC3D software. In the study, nine different rock specimen were used and the energy consumption of the crusher was compared to the results obtained using Bond's Index method. It was concluded that Bond approach was not ideal for predicting single particle fracture energy. However, in the research, the DEM rock models used were cubic and spherical in nature and this might have influenced the results as rocks are usually irregular in nature.

Cleary and Sinnott (Cleary & Sinnott, 2015) used a DEM breakage model to study a wide range of existing compression based crushers such as cone crusher, jaw crusher and gyratory crusher. The breakage model used was based on fracture of particles as they flow through the crushing chamber. Particle Replacement Model (PRM) was employed and predictions for power, product size, crusher wear and flow rates were made. PFC3D software was used. Even though DEM was found to be a powerful for prediction of the comminution process, use of PRM did not capture the dynamics of the daughter particles after breakage.

Discrete Element Method was also used by Delaney (Delaney, Morrison, Sinnott, Cummins, & Cleary, 2015) in simulation of the flow and breakage process of non-spherical particles in a cone crusher. The contact forces were calculated using a linear spring dashpot. The actual particle shape was crucial in realistic modelling of packing and flow properties of the particles. Super-quadrics were used in which the particle shaped varied randomly between blocky and rounded shapes. DEM was also used to predict the cone-crusher wear rate i.e. normal power indicated the impact damage on crusher liners while shear power indicated the abrasive damage to liners. It was concluded that DEM is ideal for predicting the particle flow, particle distribution and also the wear of comminution machines. However, the operational parameters of the cone crusher were not varied and optimisation of the comminution process was not conducted.

Potyondy and Cundall (Potyondy & Cundall, 2004) proposed a numerical model for a rock which is represented by dense packing of circular or spherical particles with different sizes. The particles were bonded together at contact points and their behaviour during comminution was simulated using DEM in both two-dimension and three-dimension. Particle Flow Code software was used. Strength parameters and stiffness were the micro-properties used for bond and particle modelling. The fracture was depicted by the broken bonds. Granite and gneiss rock were modelled using BPM in the research. It was concluded that BPM approximated the mechanical

behaviour of rocks by representing them as cemented granular materials. Particle size was also found to play a major role in a material's fracture toughness. Cho et al. (Cho, Martin, & Sego, 2007) used DEM to investigate the behaviour of rocks under compressive loading. It was found that the code used in determining the micro-parameters from uniaxial tests could not be used in predicting the intact rock response regardless of the stress path unless significant modifications were made. The research revealed that adjusting particle parameters had little effect on the macro-scale properties of tensile and compression tests. However, a methodology of measuring the energy efficiency of comminution machines was not done and only regular shaped rock models were adopted.

Litcher et al. (Lichter, Lim, Potapov, & Kaja, 2009) conducted an extensive research on how 3D discrete element method can be used to study how different cone-crusher parameters affect comminution with actual rock mechanics . The standard DEM approach cannot be applicable to systems in which size reduction is a crucial element in particle flow. Litcher developed a breakage model using Population Balance Modeling (PBM) technique to describe breakage as a function of the applied loads for different loads. In the PBM technique used, randomly shaped convex polyhedral particles were used. If the contact energy of a particle is enough to break the particle, the particle is broken instantaneously into smaller sizes whose sizes are calculated from solutions of a set of ordinary differential equations. However, each of the new particles will then behave as an independent particle. This makes PBM inferior to Bonded Particle Model as it does not fully describe the particle load-deformation profile (Jiménez-Herrera et al., 2017) and dynamics from the parent particle were lost after replacement.

Refahi et al. (Refahi et al., 2010) used DEM technique to model the fracture of a single cubic and spherical rock in a laboratory jaw crusher. The modeling involved use of granular assemblies located between the fixed and swing jaws of the crusher . The fracture energy obtained from PFC3D software simulations was compared to

experimental values. It was found that there is a good agreement between simulation values and experimental values. However, the research aimed at predicting the crushing energy of spherical rocks but not irregular shaped rocks. Fracture of cubic rocks was not well simulated using DEM.

Quist (Quist, 2012) used DEM to develop a virtual environment in which the crushing process of a cone crusher was to be simulated . Experiments were conducted on an industrial scale cone crusher to measure machine and operating conditions. Rock profiles to be used in the simulation were scanned from real rocks and exported to EDEM software for simulations. The diameter of the spheres used to create the BPM rock in the simulation varied from 3.3 mm to 12.2 mm. This brought in the aspect of heterogeneous nature of rocks. It was concluded that DEM is a powerful tool for predicting the mass flow rate and pressure comminution machines. In addition, the use of BPM rock model was highly recommended for future research in comminution.

Huiqi et al. (H. Li, McDowell, & Lowndes, 2014) used particle replacement model (PRM) to model the performance of a cone crusher during size-reduction . The breakage criterion was defined by the critical octahedral shear stresses induced in the particle. The number, size and breakage criterion was determined from experimental data obtained from compression tests conducted on a series of granite rocks. Machine parameters such as eccentric speed and closed side setting (CSS) were varied and their effect on particle size distribution were investigated. The breakage function created assumed that the original particle was to split into three particles. This is usually not the case as rocks fracture multiple times during comminution. In addition, the tensile strength, size effect factor and Weibull modulus were found to characterise the particle strength. Barrios et al. (Barrios, Tavares, & Pérez-Prim, 2015) modelled DEM simulation of particle bed compression using PRM. A comparison between unbreakable spheres and PRM during compression was made. It was concluded that DEM simulation can be used to predict the fracture of discrete particles. However, measurement of new surface area created after breakage was not possible due to the

absence of bonds in the rock model.

Cleary et al. (Cleary, Sinnott, Morrison, Cummins, & Delaney, 2017) analysed the effects of material properties on cone crusher performance using DEM . Non round particles and a breakage function were used to analyse the breakage behaviour and operating performance of a cone crusher. The breakage function used the PRM. It was concluded that increasing particle strength increased the fineness of the product generated but decreased the throughput. Particles with higher strength values tend to absorb more energy before fracturing hence break more severely generating finer product. The DEM model used was able to predict the net power draw for different material properties and operating conditions. However, the regions experiencing abrasion were not clearly defined due to the absence of bonds in rock cluster.

Pelessone et al. (Pelessone, Baum, Löhner, Charman, & Baylot, 2003) conducted a convergence study of discrete particle method (DPM), which is a class of DEM, in elastic particles. DEM is not based on continuum mechanics hence conventional convergence properties, such as FEM, will not be applicable. Vibrations of a concrete beam in free space were used as the benchmark problem. It was concluded that DPM converged to the equivalent finite element solution. However, most DEM software such as ROCKY, EDEM and PFC3D do not show the convergence of the solution. Instead, the software is already pre-calibrated to offer converged results. For instance, EDEM software automatically gives a range for the time-step and grid cell size to be used in a simulation. If the user goes outside this range, the simulation collapses (EDEM, 2012).

2.6.2 Wear Distribution using DEM

In EDEM software, the default contact model is Hertz-Mindlin (No Slip). This is due to its accurate and efficient force calculation. The force component used in Hertz-Mindlin (No-Slip) is based on Hertzian contact theory (EDEM, 2012).

Two models are used in calculating wear in EDEM - Relative wear model and Hertz-Mindlin with Archard Wear model.

The Relative wear model identifies regions of high impact (normal) and abrasive (tangential) wear on equipment. It is calculated based on the relative velocity and associated forces between the bulk material and the equipment. The properties of relative wear are Normal Cumulative Contact Energy, Tangential Cumulative Contact Energy, Tangential Cumulative Force and Normal Cumulative Force. Normal and Tangential Energy measure the cumulative energy due to material impacting and sliding respectively (DEM Solutions, 2016):

$$E_n = \sum |F_n V_n \delta t| \quad \text{when } V_n < 0, \tag{2.35}$$

where F_n is the normal cumulative force and V_n is the normal relative velocity and is negative in a loading condition. For tangential energy measure (DEM Solutions, 2016):

$$E_t = \sum |F_t V_t \delta t|, \tag{2.36}$$

where, V_t is the tangential relative velocity.

Hertz-Mindlin with Archard Wear model gives an estimation of the wear depth for geometry surfaces. It works on the idea that the amount of material removed from a surfaces is proportional to the frictional work done by particles moving over the surface (DEM Solutions, 2016). The Archard equation is given as (EDEM, 2012):

$$Q = W F_n d_t, \tag{2.37}$$

where, Q is the volume of material removed, d_t is the tangetial distance moved and W is the wear constant.

2.7 Single Particle Breakage

Comminution is considered as a series of multiple single particle breakage. However, it is impossible to calculate the internal stresses of a single irregular shaped particle subjected to compressive force (Quist, 2012). During compression of an irregular shaped rock, the number of contact points between the rock and compressing plates will depend on the shape and particle orientation. Refahi (Refahi et al., 2010) modelled spherical and cubic specimens using PFC3D software in order to determine the internal stress distribution during comminution.

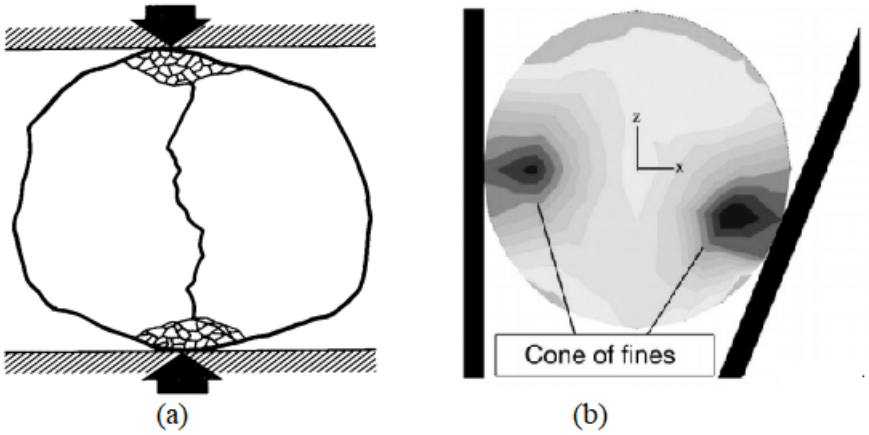

Figure 2.11: Particle under compressive loading and crack initiation (Donovan, 2003; Suresh, 2009)

As illustrated in Figure 2.11(a) and 2.11 (b), fracture starts at the contact point between the rock and crushing plates. During comminution, the major principal tensile stresses are formed within the rock particle but the areas in contact with the plates experience shatter fracture(Refahi et al., 2010). The shatter fracture is due to the excess energy input. At the contact points, abrasion is experienced because, at this time the energy input is not enough to shatter the entire particle but can only generate attrition at the loading point (Donovan, 2003).

During comminution, the feed material is in contact with the crushing plates and

this results in wear. Wear in jaw crusher liner has been studied in the past using Finite Element Method (Quartey, Njoroge, & Kihiu, 2017). However, since rocks are discrete particles, study of wear using continuum approach might yield inaccurate results. Therefore, authors have began adopting Discrete Element Modelling in wear analysis (Quist, 2012; Rojas, Vergara, & Soto, 2019; Rosales-Marín, Andrade, Alvarado, Delgadillo, & Tuzcu, 2019; Xu, Luo, & Zhao, 2018). Ramalho (Ramalho & Miranda, 2006) investigated the relationship between wear and dissipated energy in sliding systems. It was concluded that there is a direct relationship between wear and dissipated energy. The energy approach was found to be superior to other methods in that it can be applied to thin-coated surfaces even without attaining a steady state phase.

2.8 Summary

Jaw crushers are primary comminution machines which crush rocks by application of compressive forces. The size of a jaw crusher is defined by the width and gape of the machine. Size reduction in a jaw crusher is usually a series of single particles breaking until they are small enough to fit through the CSS. A lot of work has been done to increase the jaw crusher capacity and improve the product quality. However, little has been done to improve the jaw crusher energy efficiency.

Obtaining a model which takes into account all the parameters affecting the power draw of the jaw crusher is next to impossible. Therefore, using the Rose and English model, the optimal operating parameters of a single toggle jaw crusher can be obtained. This model has been adopted for this research as it has been accepted universally and involves Bond's work index in power calculation.

The most common rock strengths are compressive strength, tensile strength and shear strength. According to research work that has been done, rocks will easily fracture when subjected to tensile loading. This implies that rocks will always fail

in tension even when under compressive loading. In addition, larger rocks are easily fractured than small rocks. This is due to the presence of inherent cracks and the probability of formation of a critical flaw. In large sized rocks, the probability of occurrence of a critical flaw is higher than in small rocks.

Fracture toughness is a material property while rock strength is a function of crack length hence not a material property. However, it is challenging and more costly to measure fracture toughness than strength. A relationship between rock strength and fracture toughness was therefore developed as shown in Equation 2.18.

During comminution, the feed material is reduced in size while number of new surfaces on the feed material increase. Since fracture toughness is directly proportional to the strain energy release rate. Therefore, energy efficiency can be measured by measuring the surface area before and after comminution. For the new surfaces to be created, the strain energy release rate must be greater than the critical strain energy release rate.

Discrete Element Method is a numerical method which is ideal for simulating fracture process of discrete matter. DEM has been used by various authors to predict the fracture of rocks, power draw and ideal operational parameters of comminution machines. DEM can also be used for simulating industrial scale machines together with CAD software. Other optimisation techniques such as Genetic Algorithms and ANFIS models have been developed by various authors.

There are three major techniques of simulating particle breakage in DEM; Bonded Particle Model (BPM), Particle Replacement Model(PRM)and Population Balance Model (PBM)/Fast Breakage Model (FBM). Bonded particle model is the superior technique as it takes into account the dynamics of the fractured rocks within the simulation domain.

Discrete element method, even though ideal for simulation of discrete matter, is a

power intensive numerical method. Therefore, during calibration of the rock models, the number of particles in a cluster and particle sizes have to be regulated. This is why the diameters of spheres making up a DEM rock model vary between 2 mm and 35 mm.

Relative wear can also be obtained using DEM. During comminution, the particles exert normal and tangential forces on the liners of the size reduction machine. Some authors have used discrete element method to predict regions that experience high wear rates in a comminution machine.

From literature, the following gaps were identified;

1. The effect of throw, reduction ratio and toggle plate frequency on energy efficiency has not been studied.
2. Only circular or spherical particles have been used in modelling comminution of a jaw crusher. Irregular shapes should be used in order to mimic the real life crushing.
3. Researchers have not optimised the jaw crusher operational parameters such as the throw, reduction ratio and toggle speed. Only energy assessment has been done.
4. Interaction between the rocks and crusher liners, and wear distribution has not been studied using DEM.

This research will address all the gaps mentioned above.

CHAPTER THREE

METHODOLOGY

In this chapter, the steps applied in energy optimisation of a single toggle jaw crusher during comminution are presented. This chapter will be broken down as follows:

- Rock modelling
- Jaw crusher modelling
- Design of Experiment
- Simulation of the comminution process
- Interaction between the rocks and jaw crusher liners
- Validation

3.1 Rock Modelling

As mentioned in Chapter 2, discrete element method is a powerful numerical technique for simulation of discrete matter. There are many DEM software available but not all of them can model irregular shaped rocks. In this research, EDEM software was used in modelling an irregular shaped granite rock. EDEM (Experts in Discrete Element Method) is a simulation software developed by Altair Engineering Corporation. EDEM can be used in simualtion of granular and bulk material. Granite rock was chosen due to its mechanical properties such as high uniaxial compressive strength, elastic modulus and fracture toughness (Cleary et al., 2017; Lee, Kwon, Kim, & Cho, 2008; Refahi et al., 2010; Tromans, 2008). Other rock types, such as limestone, can also be used in simulation of comminution but the strength of the bonds created is too weak (Legendre & Zevenhoven, 2014).

3.1.1 Creating the Particle Bed

A rock is considered to be a cluster of millions of discrete elements which have different crystalline structures and minerals of varying mechanical properties. Therefore, when modelling a rock, the heterogeneity property must be well defined. Hence, different particle beds were created with the aim of getting the best heterogeneity properties. In addition, the particle bed was used in exporting particle positions for the irregular shaped rock.

In EDEM, particles are generated from factories. The factories are developed from selected geometries; flat, cylindrical and box geometries are most ideal in EDEM. Particle factories are the ones which determine when, where and how particles appear during the simulation. Any physical surface or volume can be turned into a particle factory.

There are two types of particle factory; *Static* and *Dynamic*. In static factories, the particles are produced at a specific time and simulation pauses during particle creation. In a dynamic factory, particles are created as the simulation continues. The number or mass of particles in a dynamic factory can be; unlimited or specified (by either particle number or mass). Therefore, the static factory was selected for creation of particle beds in this research. However, it was observed that static and dynamic factories were not capable of creating a BPM rock model and hence *custom factories* have to be implemented. The custom factories were created using EDEM API. In this research, static and custom factories were used as they did not demand high computational power.

The particle sizes were defined in the Particles pane in EDEM. The sizes of the particles can be fixed, random, normal and log-normal distribution (EDEM, 2012). The sizes of the particles created by custom API factories were determined by the scaling factor. During rock modelling in EDEM software, the main objective is

to grasp as many features of a real rock as possible. Therefore, the most ideal way is modelling each mineral grain, atom or molecule. Unfortunately, due to computational constrain, there is always a trade-off between the number of particles created and number of particles in a cluster. Modelling the fracture process of rock particles is best done using bi-modal distribution in which large particles are 'glued' together by smaller particles (Quist, 2012).

In creating the first particle bed, the particle sizes were varied from 2 mm to 10 mm in diameter. During the bed formation, the created particles were allowed to settle down without any additional compression as shown in Figure 3.1.

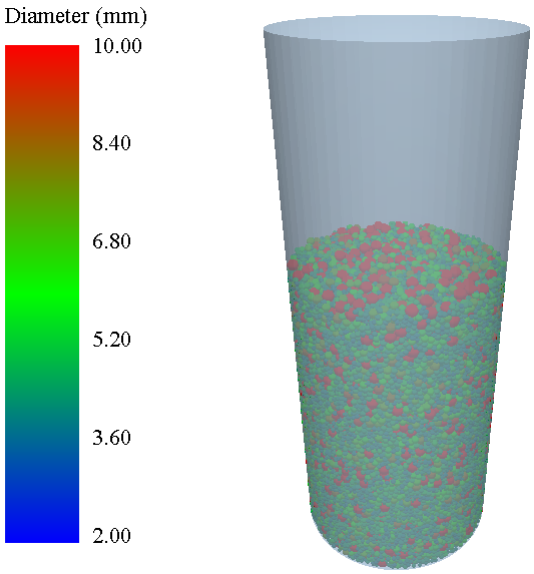

Figure 3.1: Creation of particle bed

In the second particle bed, the particle size was fixed at a diameter of 5 mm. This was done in order to investigate whether using a bi-modal distribution will have an impact on the rock's heterogeneity as shown in Figure 3.2 (i) . The third particle bed reduced the diameters of the smaller particles to 0.96 mm as shown in Figure 3.2 (ii). This was done in order to investigate the effect of changing particle sizes on heterogeneity.

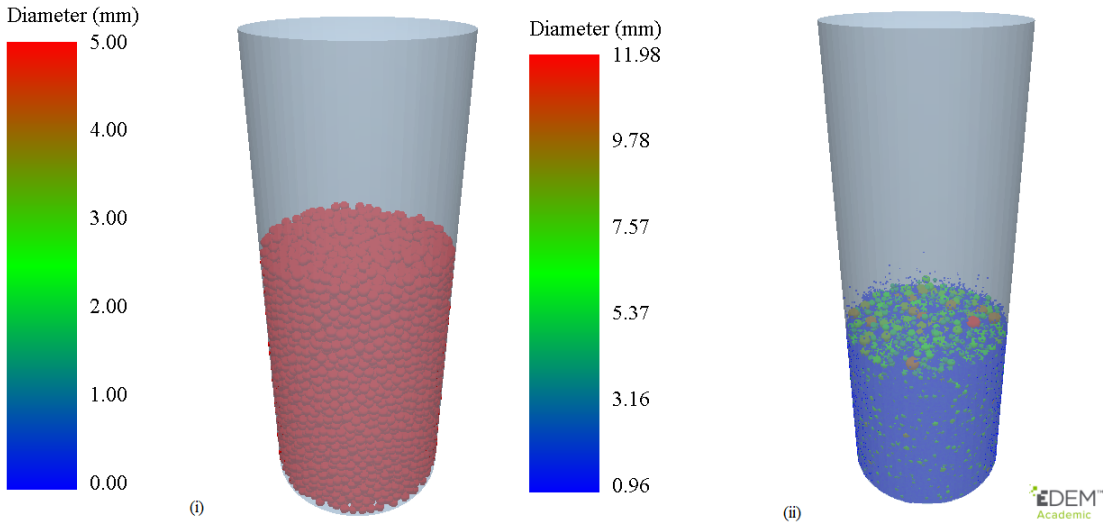

Figure 3.2: Particle beds with; fixed particle size (i) and finer particle sizes (ii)

The heterogeneity property of the particle beds was investigated using the contact vector feature. In addition, the contact radius of the particles was set slightly higher than the maximum radius of the particles i.e. for a bed whose maximum particle size had a radius of 5 mm, the contact radius was set to 5.5 mm.

3.1.2 Creating the Bin

Modelling an irregular shaped rock in EDEM software required the use of an irregular shaped bin. The imported bin was essential in selecting particle positions and sizes. To create an irregular shaped bin, spheres with diameters of 100 mm, 80 mm and 70 mm were created in AUTODESK INVENTOR and Free Form feature was used to re-shape the spheres. The aspect ratios of the irregular shaped bins are as shown in Table 3.1. The 3D and 2D shapes of the bins are as shown in Figure 3.3.

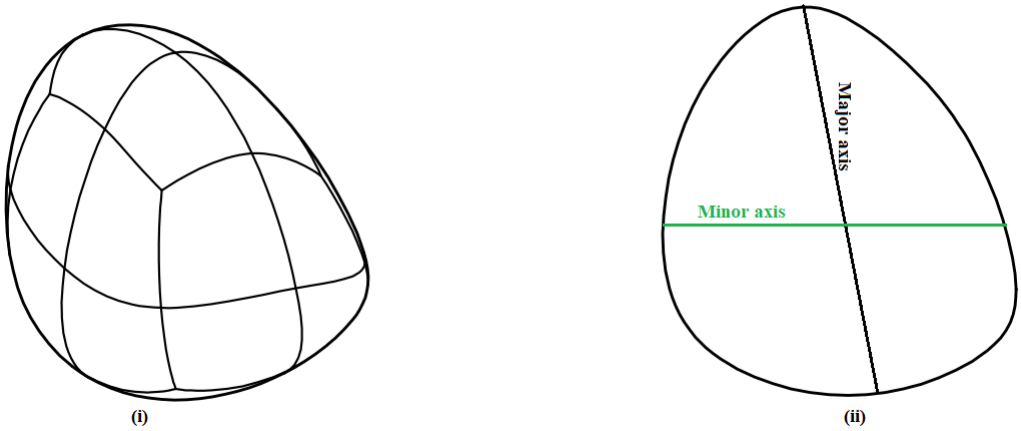

Figure 3.3: Geometry bin created using Free Form: (i) 3D view (ii) 2D view

Table 3.1: Particle bin sizes for proposed rock models

Particle Bin	Major axis (mm)	Minor axis (mm)	Aspect Ratio
X	68.86	58.02	1.187
Y	87.1	79.53	1.095
Z	94.84	87.69	1.082

3.1.3 Importing the Bin to EDEM and Obtaining Particle Positions

The bin created in Figure 3.3 was imported to the particle bed shown in Figure 3.1. The bin is automatically placed at the centre of the cylinder i.e. at co-ordinates (0,0,0) in global x,y,z axes. Therefore, the particles had to completely cover the bin to ensure that all particle positions for the BPM model are obtained. Figure 3.4, from the left, shows the steps taken to obtain the total number of particles in cluster and their respective positions.

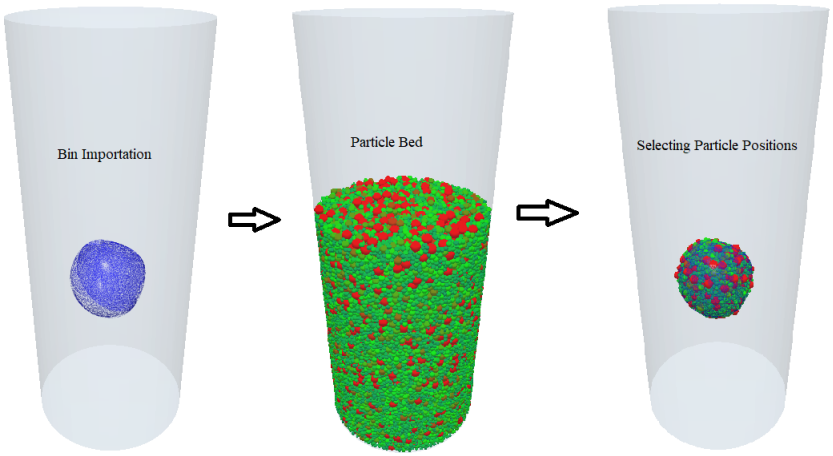

Figure 3.4: Obtaining total number of particles and respective positions in cluster

3.1.4 Creating the BPM Rock Model

The BPM rock model required the creation of custom factory using EDEM API(Application Program Interface). Therefore, a *Meta-Particle* was introduced into the simulation. The *Meta-Particle* was replaced by individual spherical particles bonded together at positions relative to the local axis of the *Meta-Particle*. Figure 3.5 shows the process used to create the BPM rock model. Appendix B shows more information regarding the files used in custom API creation.

Figure 3.5: Creating the BPM rock model

The *Particle cluster data* contained the diameters and total number of particles in the rock model together with their respective positions relative to the local axis of the

Meta-Particle. The data obtained in Figure 3.4 in EDEM was exported to Microsoft Excel and re-arranged in the following way:

Number of particles in cluster

X1	Y1	Z1	SF1
X2	Y2	Z2	SF2
X3	Y3	Z3	SF3
...			

where, the particle positions in local *xyz-axis* were in columns 1 to 3 and the particle diameters were in column 4. The particle diameters were used as the scaling factor of each particle during BPM rock model so as to attain high heterogeneity. The total number of particles in cluster were used in creation of *Custom API file* in Visual Studio 2012 as shown in Figure 3.6.

```
//Add the name for the custom property and preference file name
const string CCustomFactory::PREFS_FILE = "Particle_Cluster_Data.txt";


//initialise variables
int particles_to_create = 0;
int CNum = 2527;                    //number of particles in cluster
double **arrCPos;                 //array for positons of particles within cluster
bool Factory_Used = false;        // Check the custom Factory has created in the simulation
int CCreate = 0;                  //Cluster element currently being created
```

Figure 3.6: Creation of custom factory file in Visual Studio 2012

In Figure 3.6, the *Particle Cluster Data* is called and the total number of particles are 2527. This data was for Particle Z. To replace the *Meta-Particle* with individual spherical particles, the replacement time had to be defined in *Particle Replacement File*. The *Custom API file* was finally created and was used as the custom factory. The files used in creating the custom API are present in the APPENDIX.

In EDEM, the mechanical properties of the granite rock were required in order to create the BPM model. The mechanical properties used are as shown in Table 3.2.

Table 3.3 shows the DEM material properties used.

Table 3.2: Bonded particle model parameters (Quist, 2012)

Parameter	**Value**	**Unit**
	BPM Parameters	
Normal Stiffness per unit area	1670	[GN/m^3]
Shear Stiffness per unit area	667	[GN/m^3]
Shear Critical Stress	24	[MPa]
Normal Critical Stress	36	[MPa]
Bond disc radius	5.5	[mm]

Table 3.3: DEM material properties (Quist, 2012)

Property	**Rock**	**Steel**	**Unit**
Density	2630	7800	[Kg/m^3]
Poisson's Ratio	0.35	0.3	[-]
Shear Stiffness	5.571e8	7e10	[Pa]
	Rock-Rock	**Rock-Steel**	
Coefficient of static friction	0.5	0.7	[-]
Coefficient of restitution	0.2	0.25	[-]
Coefficient of rolling friction	0.001	0.001	[-]

In EDEM, a *Meta-Particle* named $Whole$ was created and its diameter was slightly higher than the average rock diameter. A second particle named $Fraction$ was created and this was to replace the *Meta-Particle* to form the BPM rock model. The size distribution for the $Fraction$ particle was fixed at a radius of 1 mm and BPM parameters shown in Table 3.2 were added to this particle. However, due to computational power limitations, creating a BPM rock model using Particle Z with a cluster of 2527 particles was not possible. Therefore, smaller sized rock models were proposed. Creating a BPM rock using Particle Y whose cluster had 1661 particles also demanded a higher computational power for it to be simulated. On the other

hand, creating a BPM rock using Particle X whose cluster had 764 particles did not demand a lot of computational power hence was picked for size-reduction simulations.

The steps involved in creation of the BPM rock model in this section are summarised as:

(i) Two cylinders of suitable diameter and height were created. The dimensions and positions of the cylinders in xyz axes were selected such that the particles created would completely surround the imported geometrical bin.

(ii) One of the cylinders was set to be the factory while the other, the container.

(iii) Particles were created and let to settle forming a loosely packed bed as shown in Figure 3.4.

(iv) Using the selection bin group, as shown in Figure 3.4, the number of particles, particle positions and diameters in meters were saved in text file format.

(v) The number of particles in the clusters was used in C++ code. The code was later used in EDEM software as a custom API.

(vi) The total number of particles and particle positions were re-arranged in the following way. This was done to ensure that EDEM software calls each particle position and its size during simulation.

```
764
0.000455    -0.00069    0.0012      5
0.000519    -0.00117    -0.00265    2.4985
-0.001624   0.00105     0.000056    4.121655
...
```

3.2 Jaw Crusher Modelling

As mentioned in Chapter 1, the main objective of this research is to optimise the energy efficiency of a single toggle jaw crusher. The jaw crusher shown in Figure 1.1 was used in comminution simulations. The dimensions and operational parameters for the unoptimised jaw crusher are as shown in Table 1.1. Selection of operating parameters and dimensions was guided by the Rose and English model (A. Gupta & Yan, 2006) and the work of Legendre and Zevenhoven (Legendre & Zevenhoven, 2014). In energy optimisation, the throw, reduction ratio and toggle speed frequency were the only parameters considered as they are functions of power which could be varied (A. Gupta & Yan, 2006). In Figure 3.7, the *Meta-Particle* is fed into the full scale jaw crusher for simulations. It can be observed that the *Meta-Particle* for Particle X is very small in comparison to the jaw crusher dimensions. This means that crushing will probably start near the close side set (CSS) of the crusher or the particle might pass through the crushing chambers un-crushed.

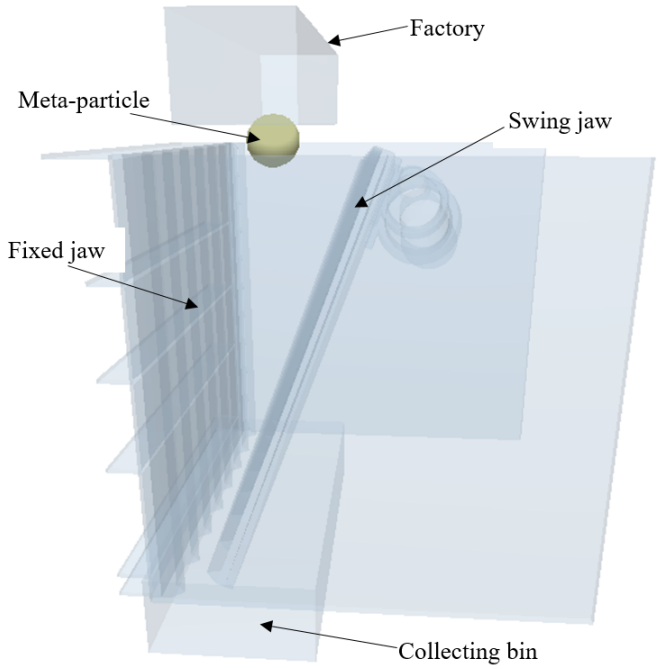

Figure 3.7: Simulation in a full-scale sized jaw crusher

In Figure 3.7, the simulation results will not be realistic as breakage will start at the bottom-most part of the jaw crusher. In Figure 3.8, it is shown that the comminution process will start near the top section of the crushing chamber. Therefore, there is need to scale down the crusher so that crushing starts near the top section of the crushing chamber. In addition, increasing the particle size was impossible due to computational limitations. For instance, creating a BPM rock model of an average diameter of 80 mm required an additional 32 GB of Random Access Memory (RAM) for the simulation to take place.

Scaling down the crusher will affect the length and consequently affect the throw. However, it will not have an impact on toggle speed frequency, reduction ratio and total energy efficiency as these parameters are not dependent on length. According to Gupta (A. Gupta & Yan, 2006), the feed size should be approximately equal to 0.8 - 0.9 of the gape size and hence, in this research, the jaw crusher was scaled down by 50% and the resulting jaw crusher model is as shown in Figure 3.8.

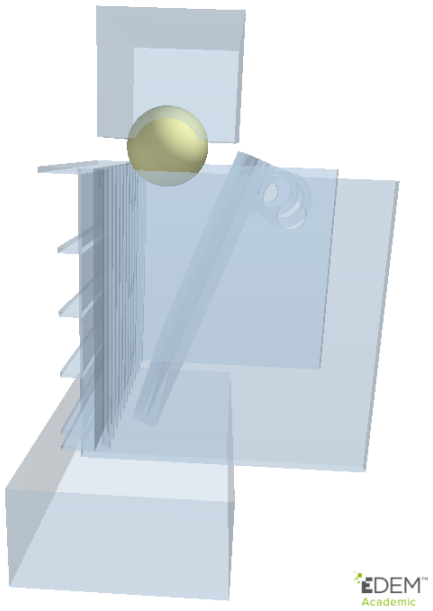

Figure 3.8: Simulation in a scaled-down jaw crusher

The new jaw crusher dimensions which were used in the simulation are shown in Table 3.4. After the simulations and data analysis, the scaled-down jaw crusher was scaled up to its original size. This was done using the Genetic Algorithm code. In addition, the reduction ratio and toggle speed frequency were not scaled down as they are not functions of length. However, the throw was scaled down.

Table 3.4: Scaled-down jaw crusher parameters

Parameter	Dimension	Unit
Gape	0.1175	m
Width	0.235	m
Length	0.25	m

3.3 Design of Experiment(DOE)

During size-reduction in a single-toggle jaw crusher, three variables which affect power consumption can be combined in any way. For instance, if the toggle speed is to be varied from 100 rpm to 300 rpm in steps of 1 rpm, the throw varied from 5 mm to 35 mm in steps of 5 mm and reduction ratio from 4 to 7 in steps of 1 unit, then there would be a total of 211 intervals. Using combinations and permutations:

$$C(n,k) = \frac{n!}{k!(n-k)!} = \frac{211!}{3!(211-3)!} = 1543465, \tag{3.1}$$

where, n is the total number of intervals and k is the number of variables. From Equation 3.1, the required number of simulations obtained were 1543465 which are near impossible to conduct due to time constraint and computational power. Combinations were used in Equation 3.1 since the variables could combine in any random order.

Therefore, MINITAB software was used to determine the best number of simulations

and combinations. Using DOE, the interaction between reduction ratio, toggle speed frequency and throw with energy efficiency was investigated. A relationship between the energy efficiency and jaw crusher operating parameters was also developed. Table 3.5, eight runs with variable throw, reduction ratio and toggle speed were to be conducted.

Table 3.5: Number of runs used in the simulation

Run	Throw	Reduction Ratio	Toggle Speed
1	35	4	300
2	35	7	300
3	35	7	100
4	35	4	100
5	10	7	300
6	10	7	100
7	10	4	300
8	10	4	100

Full Factorial experimental design was used to develop the values in Table 3.5. In this research, there are three variables and each of them has a lower bound and an upper bound. Therefore, by using Equation 2.29, the number of runs were found to be equal to $2^3 = 8$. The simulations runs were conducted in the order shown and energy efficiency for each run was recorded and used for analysis.

3.4 Obtaining the Total Energy Efficiencies

Guided by Equation 2.26, the new surface area created, $A_{Created}$, was obtained from the number of bond broken in that the new surface area is given by $2\pi N_B r$ where N_B and r are number of bonds broken and the bond radius respectively. The fracture surface energy, γ, was obtained from a the gradient of the graph of the cumulative energy of the swing jaw versus the new surface area created. The particle mass M was obtained from EDEM software. The limiting efficiency η_{Limit} was calculated

using Equation 2.24.

3.5 Genetic Algorithm

A GA code was used in this research work to obtain the highest possible efficiency. The equation obtained from the relationship between the process parameters and energy efficiency was used as the objective function in the GA and was maximised. The global or maximum value of efficiency from the GA was selected as the target value in DOE. The GA code was also used to minimize the objective function for the validation process. The objective function was obtained from simulations. In order for optimisation to be conducted using GA, the constraints were set set as shown in Table 3.6 as guided by Rose and English (A. Gupta & Yan, 2006). Appendix A shows the implementation of genetic algorithm in optimising the objective function.

Table 3.6: Constraints used for optimisation in GA

Parameter	**Lower Limit**	**High Limit**
Reduction ratio	4	7
Throw (mm)	10	35
Toggle speed (rpm)	100	300

In addition, the GA code was used in scaling up of the jaw crusher using Equation 2.11. Equation 2.11 is the power equation modelled by Rose and English. Power was considered as the jaw crusher size determines the power draw of the crusher. Therefore, by scaling down the jaw crusher dimensions i.e. from a scale of 0.5 to 1 in steps of 0.1, a relationship between consumed power and scaling factor was obtained. However, before the upscaling was conducted, the critical velocity was obtained using Equation 2.4 so as to determine the actual flow rate (Q_A) from Equation 2.5. The packing factor $f(P_K)$ was determined using Equation 4.7 and Figure 2.4. The Bond's work index (W_i)function $f(\beta)$, the surface characteristic parameter for the rock (S_C) and the ore density ρ_s were also determined. The GA parameters such as population size, number of generations and function tolerance are as shown in APPENDIX A.2.

The values of GA parameters used were selected so as to increase the accuracy of the optimisation.

3.6 Interaction Between the Rocks and Jaw Crusher Liners

During comminution, the rocks interact with the jaw crusher liners which results in wear of the liner profile. To investigate the regions experiencing wear using DEM, the Relative Wear feature in EDEM software was used. The Relative wear feature used the cumulative energy to detect regions affected by wear.

The mode of fracture was also investigated. The contact points between the rock and jaw crusher liners during the compression stroke was investigated. The normal force within the BPM rock model was used as an indicator of the stresses within the rock during and after crushing process.

Particle flow during comminution was also investigated. The velocity of the fractured particles after breakage indicated the impact of friction on flow rate. The magnitude of velocity was also used to show why some regions had higher wear rates than others.

3.7 Validation

In this research, validation of the simulation results was done from existing data (Legendre & Zevenhoven, 2014). To validate the results, the objective function obtained using DOE was minimised using Genetic Algorithm and the efficiency was compared to existing data in literature. Minimising the GA code was necessary since the author whose data is being compared to for validation also minimised the process. The BPM rock model used had granitic rock properties rather than the limestone rock properties as used by Legendre and Zevenhoven. The main reasons as to why granite rock properties were used rather than that of limestone were:

- Granitic rocks have better mechanical properties such as high fracture toughness, high uniaxial compressive strength and elastic modulus than limestone rocks (Cleary et al., 2017; Lee et al., 2008; Refahi et al., 2010; Tromans, 2008).

- Limestone rock model used by Legendre and Ron (Legendre & Zevenhoven, 2014) had weak bonds due to the DEM properties chosen. The weak bonds led to complete shatter of the model once it hit the collecting bin *i.e* the crushing process resulted in feed material which appeared to be ground rather than crushed. Legendre and Ron also pointed out that the bond properties did not have an impact on the breakage behaviour of the rock model.

According to research, the type of rock used will not have an impact on the energy efficiency but will influence the power draw of the comminution machine (Legendre & Zevenhoven, 2014). The results obtained from simulations and optimisation process were validated using existing data from literature.

CHAPTER FOUR

RESULTS AND DISCUSSION

In this chapter, the results obtained from modeling of BPM rocks and simulation of the comminution process are presented and analysed. The total energy efficiencies of different process parameters have also been presented. The objective function which relates the energy efficiency to the process parameters was also developed. In addition, the effect of each parameter on the total energy efficiency was analysed. The interaction between the rock models and the jaw crusher liners has been discussed. Regions experiencing high wear rates were detected using discrete element method. Each simulation took an average of 30 hours. The computer specifications used were: Intel Core i7-7700HQ CPU @2.80GHz, RAM 16 GB DDR4 and Graphics card NVIDIA GTX 1070.

4.1 Particle Bed

The heterogeneity of the particle beds was as shown in Figures 4.1 and 4.2. In Figure 4.1 (i), the heterogeneity aspect of the particle bed with the bi-modal distribution is represented by the various colours. The colours show the length of the contact vectors and it can be seen that the particle bed is highly heterogeneous. On the other hand, the particle bed with fixed size particles has only one colour for the contact vectors and hence this is not heterogeneous in nature as shown in Figure 4.1 (ii). In addition, due to the absence of finer particles between the coarse particles, small gaps are observable within the particle bed whose particle size is fixed.

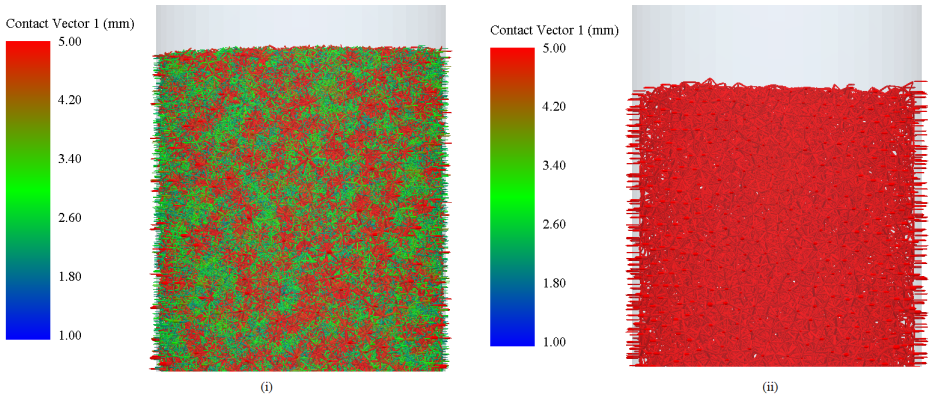

Figure 4.1: Contact vectors for (i) bi-modal distribution and (ii) fixed particle sizes

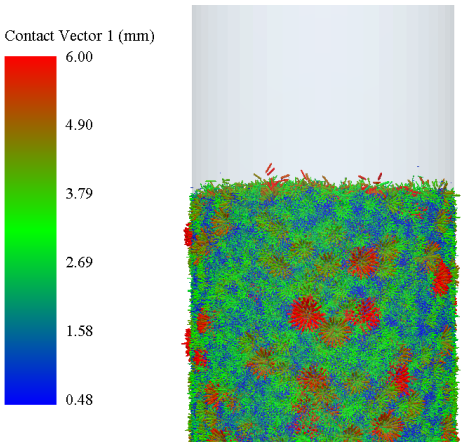

Figure 4.2: Contact vectors for particle bed with finer particles

In Figure 4.2, the particle bed is still highly heterogeneous and reducing the particle sizes only increased the computational power required but did not improve the heterogeneity of the particle bed. Therefore, using a particles sizes varying from 2 mm to 10 mm in diameter reduced the computational power and still mimic the size-reduction process.

4.2 Created BPM Rock Model

The BPM rock created is as shown in Figure 4.3. The rock model created was used in simulating the size reduction process.

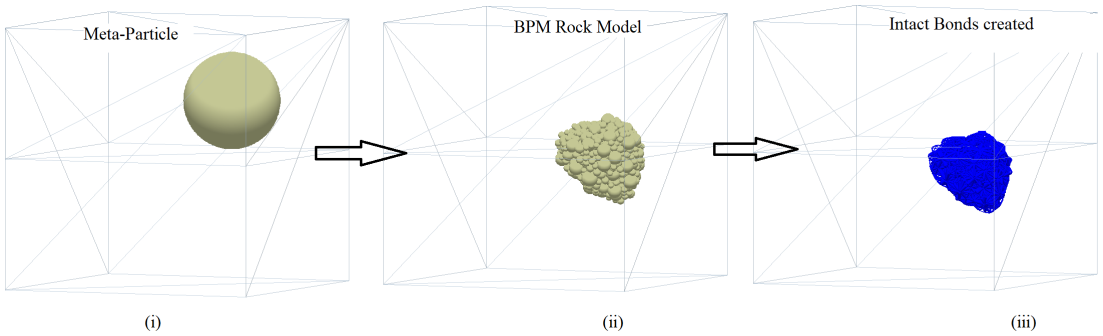

Figure 4.3: BPM rock model formation: (i) Creation of the Meta-Particle, *Whole*. (ii) Particle replacement and bond formation. (iii) Intact bonds as a result of BPM

4.3 Simulation of the Comminution Process

The simulations showing how comminution takes place in a single toggle jaw crusher were done and parameters varied as guided by Table 3.5. The crushing process starts as shown in Figure 4.4. It was observed that the maximum normal force was at the contact point between the jaw liners and the BPM rock model.

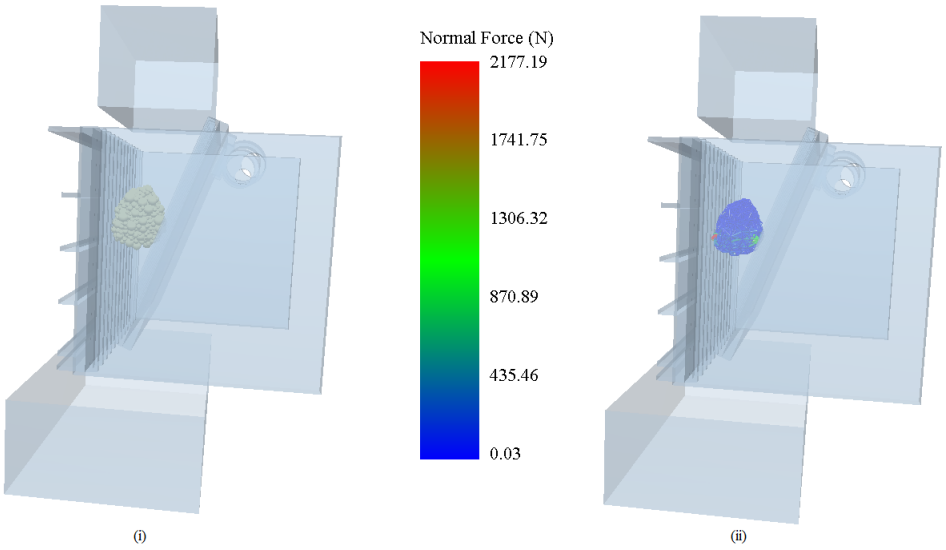

Figure 4.4: Start of comminution process:(i) Compression of BPM rock model (ii) Force distribution within the bonds

Fracture took place shown in Figure 4.5. Here, the BPM rock model is broken into two creating the products. There are residual forces within the rock and a maximum residual force of 838.9 N was recorded.

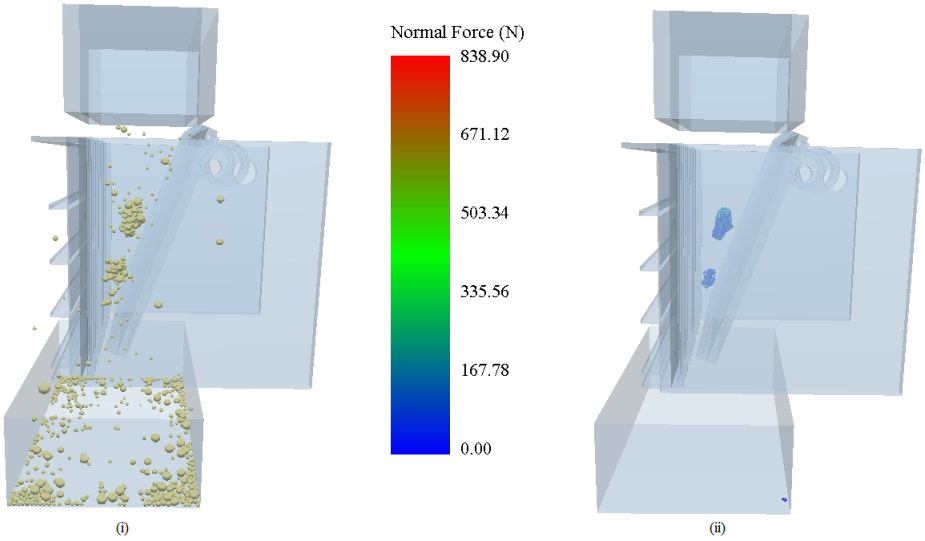

Figure 4.5: Fracturing of the BPM rock model (i) Fracture of the BPM rock (ii) Residual forces within the crushed rock

The comminution process ended as shown in Figure 4.6. It was also observed that there are residual forces within the crushed rock. The results obtained were used to calculate the total energy efficiency as guided by Equation 2.26.

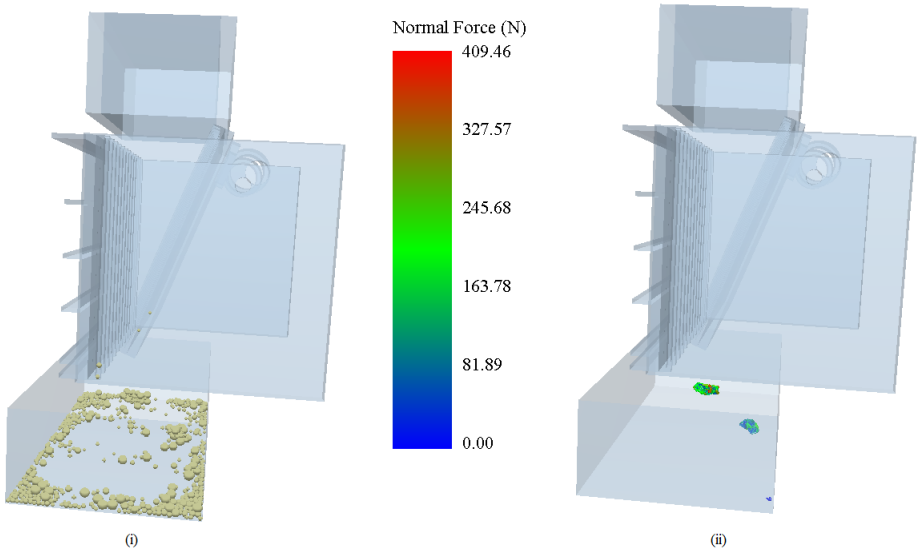

Figure 4.6: End of comminution process (i) Product and (ii) Intact bonds after comminution ends

4.4 Total Energy Efficiencies for Different Operation Parameters

The total energy efficiency was recorded as the response of the runs shown in Table 3.5 in Design of Experiment software. Table 4.1 shows the total energy efficiency values obtained from eight simulations in which *throw*, *reduction ratio* and *toggle speed* were varied.

The energy efficiency values were obtained using equation:

$$\eta_{EnergyTotal} = \frac{\gamma A_{Created}}{\eta_{Limit} ME_{Equipment}}, \tag{4.1}$$

where

- Total particle mass, M, was obtained as 0.214387 kg using EDEM,
- The limiting efficiency, η_{Limit}, was obtained as 0.0866%,

Table 4.1: Total equipment energy efficiency simulation results

Run Order	A (mm)	B	C (rpm)	Total Energy Efficiency (%)
1	35	4	300	28.1375
2	35	7	300	58.0206
3	35	7	100	54.6520
4	35	4	100	9.1187
5	10	7	300	35.6973
6	10	7	100	46.7317
7	10	4	300	42.6202
8	10	4	100	66.7484

From Table 4.1, it is evident that there is a clear relationship between the operating parameters and the total energy efficiency, $\eta_{EnergyTotal}$. Therefore, using the *Regression Feature* in MINITAB, a relationship between the input variables (*throw, reduction ratio and toggle speed*) and the response ($\eta_{EnergyTotal}$) was obtained. In addition, the value of efficiency dropped from 54.652% to 9.1187% in Table 3.5. This was due to the effect of the interactions between the parameters.

The total energy efficiency is, therefore, given by:

$$\eta_{EnergyTotal} = 188.5 - 0.3709C - 19.51B - 7.431A + 0.04099CB + 0.01629CA + 1.066AB - 0.001916ABC, \tag{4.2}$$

where, A is the **Throw** mm, B is the **Reduction Ratio** (-) and C is the **Toggle Speed** rpm.

4.5 Interaction between Reduction Ratio, Throw and Toggle Speed Frequency

The power consumption of a jaw crusher is a function of throw, reduction ratio and toggle speed frequency. There has not been a relationship between the operating parameters and total energy efficiency of a jaw crusher. However, the results in Table 4.1 indicate that there is a relationship between the input parameters (throw, reduction ratio and toggle speed) and the output (energy efficiency). Analysing the interaction between throw, toggle speed and reduction ratio made it possible to determine which parameter(s) has (have) the highest impact on energy efficiency. Using the obtained knowledge, the manufacture of jaw crushers will primarily focus on parameters which have a high impact on energy efficiency.

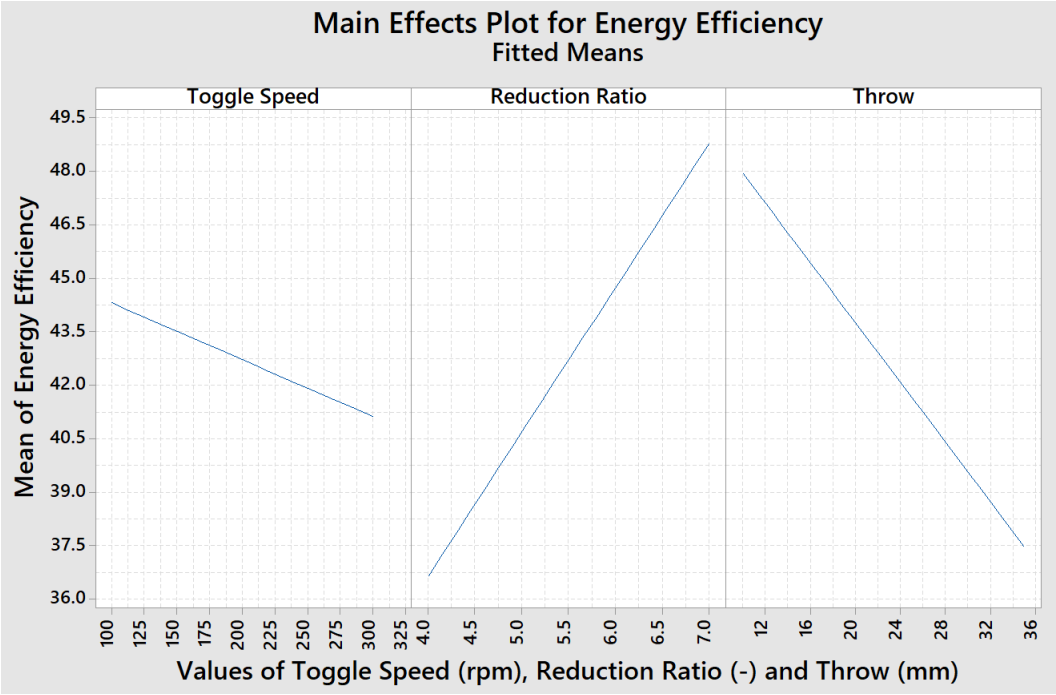

Figure 4.7: Main effects plots for energy efficiency

Figure 4.7 shows the main effects plots for energy efficiency. It is evident that an increment in toggle speed and throw results in a decrease in energy efficiency.

However, throw has a higher impact on energy efficiency as its plot is steeper than that of toggle speed. The reduction ratio, when increased, increases the energy efficiency. From the main effects plot, it is evident that the factors have an impact on energy efficiency. This was done to investigate the impact of each parameter on the energy efficiency. The linearity aspect of the graphs in Figure 4.7 was due to the fact that the process parameters only had two-levels i.e. lower and upper limits.

During comminution, the critical parameters interact with each other. For better visualisation of how these factors interact and hence influencing the energy efficiency an interaction plot is presented. In Figure 4.8, the throw interacts with all the other

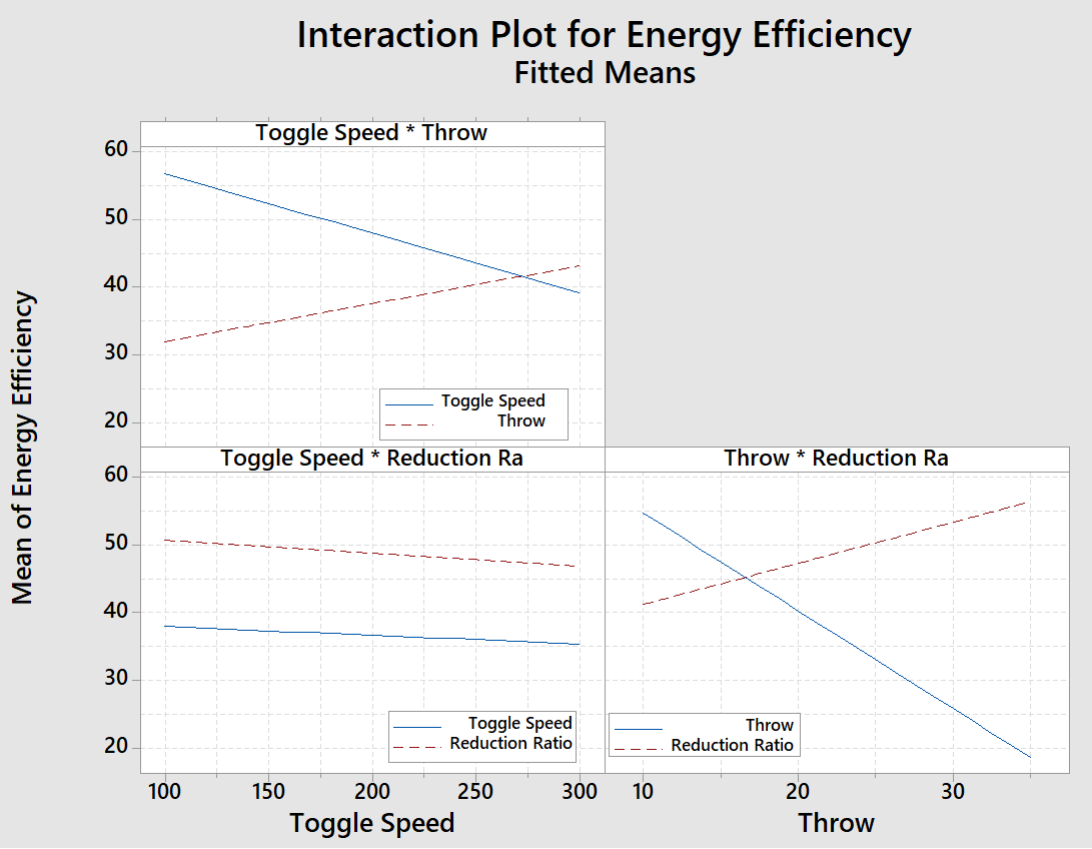

Figure 4.8: Interaction plot for energy efficiency

parameters. This is also evident in the Pareto Chart of effects presented in Figure 4.9. This is because the distance and velocity of the throw is affected by the reduction

ratio and the toggle speed. Even though the toggle speed and reduction ratio interact at some point, the interaction is weak as the lines are nearly parallel to each other. The interaction plots for energy efficiency show that there is a very strong interaction between the throw and reduction ratio due to the high slope of the lines. The graphs shown in Figures 4.7 and 4.8, however, do not show the impact of the critical process parameters on energy efficiency. Therefore, surface plots shown in Figures 4.10- 4.12 were created using objective functions obtained from MINITAB software.

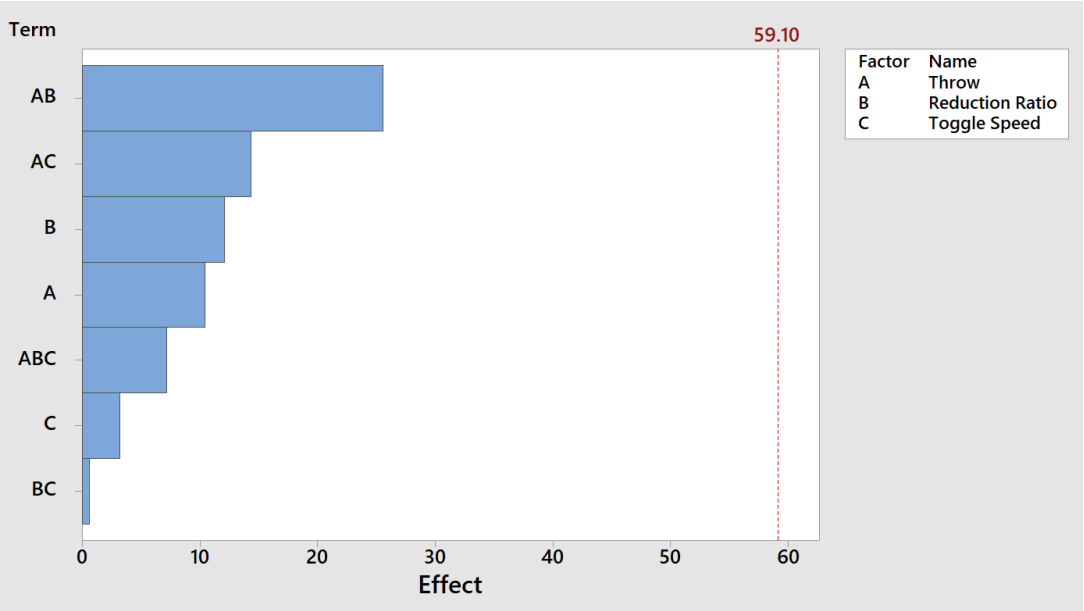

Figure 4.9: Pareto plot for effect of critical variables on energy efficiency

Figure 4.9 shows a Pareto chart which depicts the effect of individual and a combination of the critical parameters on energy efficiency. The value of alpha, α, in Figure 4.9 is 0.05 and hence there is only a 5% chance of error that the findings are incorrect. It is important to note that the Pareto chart cannot show how an increment or decrement of the factors affects the energy efficiency. A combination of throw and reduction ratio has the highest impact on energy efficiency while a combination of reduction ratio and toggle speed has the minimum effect. The reduction ratio has the highest impact on energy efficiency as a single parameter

while toggle speed has the minimum effect. This is also the reason why there is a drastic drop in efficiency between run 3 and run 4 of Table 3.5. Any change in the throw or reduction ratio is observed to have a high impact on energy efficiency.

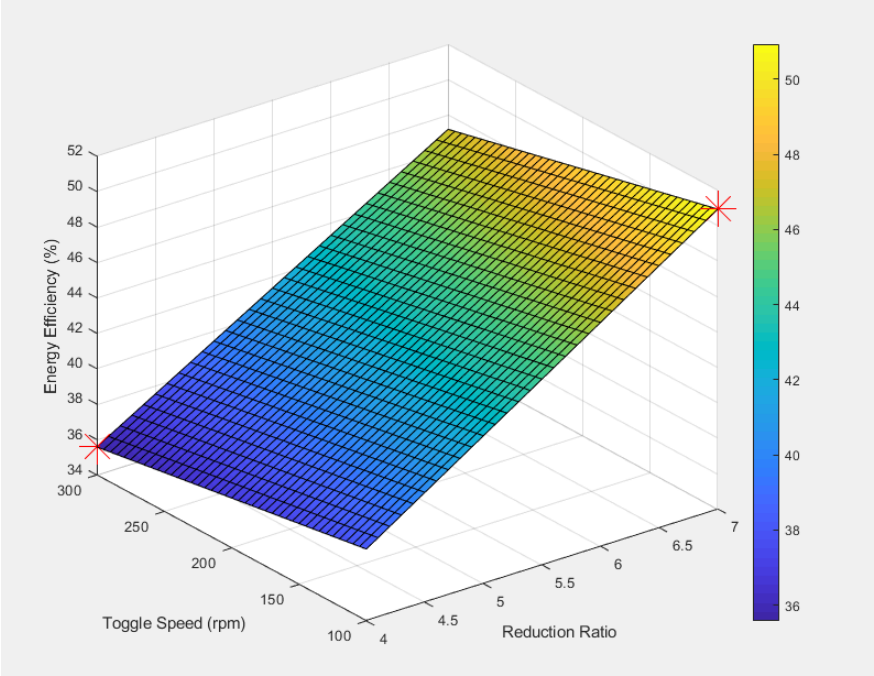

Figure 4.10: Effect of toggle speed and reduction ratio on efficiency

In Figure 4.10, the effect of toggle speed and reduction ratio on energy efficiency is investigated. The throw was held at a constant value of 22.5 mm. The maximum value of efficiency obtained is 50.93% while the minimum value is 35.58%.. This relationship was obtained using MINITAB as shown in Equation 4.3:

$$\eta_{EnergyTotal} = 21.3 - 0.004C + 4.5B - 0.0021BC. \tag{4.3}$$

The impact of throw and reduction ratio on energy efficiency was investigated using Equation 4.4 in which the toggle speed was held at 200 rpm. A plot shown in Figure 4.11 was developed and the maximum and minimum values of efficiency recorded

were; 56.37% and 18.69% respectively.

$$\eta_{EnergyTotal} = 114.4 - 11.31B - 4.17A + 0.682AB. \tag{4.4}$$

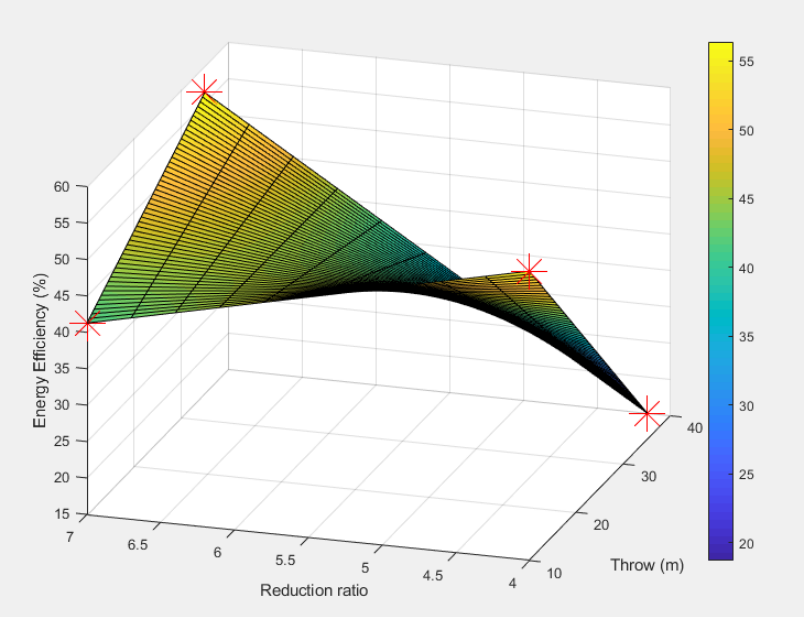

Figure 4.11: Effect of throw and reduction ratio on efficiency

A combination of throw and toggle speed yielded an energy efficiency of 56.76% and 31.91%. These values are marked in Figure 4.12 and are obtained using Equation 4.5. Here, the reduction ratio was held at a value of 5.5.

$$\eta_{EnergyTotal} = 81.2 - 0.145C - 1.57B + 0.00576BC. \tag{4.5}$$

The values of parameters held constant in Equations 4.3 - 4.5 were pre-determined by the statistical software, MINITAB. It is evident that throw and reduction have a high impact on energy efficiency i.e. they have a high and the least value of energy efficiency. This is also shown by the values in Pareto chart in Figure 4.9 as a combination of throw and reduction ratio has the largest impact on efficiency. This

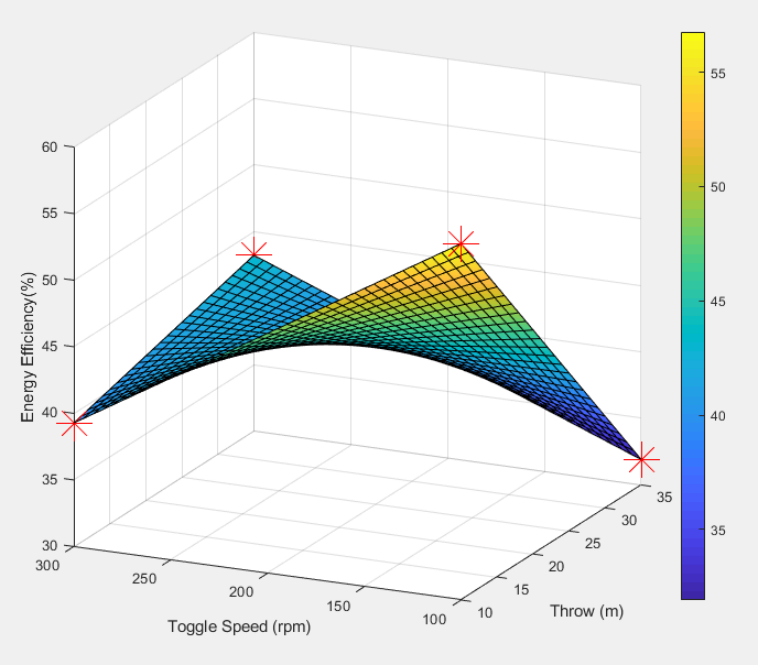

Figure 4.12: Effect of throw and toggle speed on efficiency

was because throw and reduction ratio affect the distance travelled by the swing jaw during compression. For instance, a longer compression stroke implies that more force is applied to the feed material for crushing to take place.

It was observed that the toggle speed has the minimum effect on energy efficiency. This was due to the fact that toggle speed only affects how fast the swing jaw travels but not the compression process. Therefore, decreasing or increasing the toggle speed will only affect the power consumption but not the efficiency as shown in Equation 2.11. The linear nature of the plot in Figure 4.10 was also due to the fact that toggle speed has very minimal effect on energy efficiency and since the throw was not varied, the only variable with an impact on efficiency was the reduction ratio leading to a linear output of the objective function. However, the surface plot of the toggle speed and throw as shown in Figure 4.11 was parabolic and not linear. This is because there is a strong interaction between throw and toggle speed as shown in Figure 4.8. In addition, a combination of throw and toggle speed has a high effect on energy efficiency as shown in Figure 4.9.

4.6 Validation of Simulation Results

The results obtained from the simulation of the comminution process were compared to existing experimental results by various authors. The BPM parameters used in this research and those used in Legendre's research are as shown in Table 4.2. Legendre and Zevenhoven (Legendre & Zevenhoven, 2014) assessed the energy efficiency of a jaw crusher using DEM and GA. In addition, Legendre and Zevenhoven validated their numerical model via experiments hence their simulation results were used for validation purposes in this research.

Table 4.2: A comparison of BPM rock model properties

Parameter	Used Values	Legendre
Ore	*Granite*	*Limestone*
Normal critical stress	36 MPa	59 MPa
Shear critical stress	24 MPa	29.5 MPa
Ore density	2.63 t/m^3	5.197 t/m^3
Poisson's ratio	0.35	0.2616
Coefficient of static friction (ore-ore)	0.5	0.8
Coefficient of static friction (ore-steel)	0.7	0.5
Coefficient of rolling friction	0.001	0.05
Shape of BPM rock	*Irregular*	*Spherical*
Nature of cluster in BPM rock	*Heterogeneous*	*Homogenous*

The total equipment energy efficiency obtained by Legendre was 20.9% while the one obtained in this research was 26.747%. The energy efficiency of 26.747% was obtained by minimising the objective function shown in Equation 4.2. It is observed that there is a difference of 5.847% between the energy efficiencies. This difference was brought about by the shape of the BPM rock used and also the strength of the bonds created using simulation. It is also observed that Legendre used a homogenous rock model which does not reflect the true nature of real rocks and this also affected the energy efficiency. Therefore, the objective function in Equation 4.2 can also be used to optimise the jaw crusher shown in Figure 1.1. However, in experiments,

Legendre pointed out that toggle speed had minimum to zero impact on particle size distribution during comminution while reduction ratio and throw had a high impact on size distribution of broken rocks. Size distribution is a function of the number of broken bonds which dictates the energy consumption of the jaw crusher. In this work, it was also been concluded that the toggle speed has minimum effect on energy efficiency hence the model in 4.2 was adopted. Furthermore, the type of rock used was found not to have an impact on energy efficiency of the jaw crusher (Legendre & Zevenhoven, 2014).

Khaled (Abuhasel, 2019) developed a regression model which predicted the energy consumption of a single toggle jaw crusher. It was concluded that the gape had minimum effect on the energy consumption. The reduction ratio was found to be directly proportional to the energy consumed. This is also in agreement with the results obtained from the simulations in this research work. Khaled also concluded that an increment in size of closed set setting (CSS) resulted in an increment in energy consumption. The CSS is defined by the throw and hence this justifies the findings in this research in that the throw has a high impact on the energy efficiency.

4.7 Energy Optimisation Process

4.7.1 Optimising the Scaled-Down Jaw Crusher

In Table 4.1, the maximum value of $\eta_{EnergyTotal}$ is 66.7484% while the minimum value is 9.1187%. It is evident that the parameters addressed in Table 4.1 interact with each other to affect equipment total energy efficiency. Therefore, using the response optimiser feature just to *maximise* or *minimize* the total energy efficiency would give inaccurate results i.e. if the response optimiser is set to *maximise* the efficiency, it will only take the values of Run 8 as the optimal values.

Therefore, using a genetic algorithm code to optimise the comminution process is

recommended. Using Equation 4.2 as the objective function, an optimisation GA code was used in MATLAB to obtain a maximum energy efficiency of 59.7758%. Now, in the response optimiser, a target value of 59.7758% was set and the optimal values of throw, reduction ratio and toggle speed frequency were as shown in Table 4.3:

Table 4.3: Optimal jaw crusher operating parameters

Parameter	**Optimal Value**
Throw	10 mm
Reduction Ratio	4
Toggle Speed	160 rpm

The values in Table 4.3 are for the scaled-downed jaw crusher. Therefore, an upscaling design was implemented.

4.7.2 Upscaling the Jaw Crusher to its Original Size

The maximum critical velocity was obtained using Equation 2.4 as 435.1352 rpm and is shown in Figure 4.13. Since the critical velocity, v_C, is greater than the operating velocity, v, then the actual jaw crusher capacity Q_A was calculated using Equation 4.6:

$$Q_A = Q_M \, \frac{v}{v_c}. \tag{4.6}$$

To calculate the value of Q_M, as shown in Equation 2.2, the following variables were defined:

$$P_k = \frac{70 - 70}{70} = 0 \quad \text{(used to obtain } f(P_K)\text{)}. \tag{4.7}$$

The values of $f(P_k)$, $W_i, f(\beta), S_C$ and ρ_s were:

$f(P_k) = 0.6,$

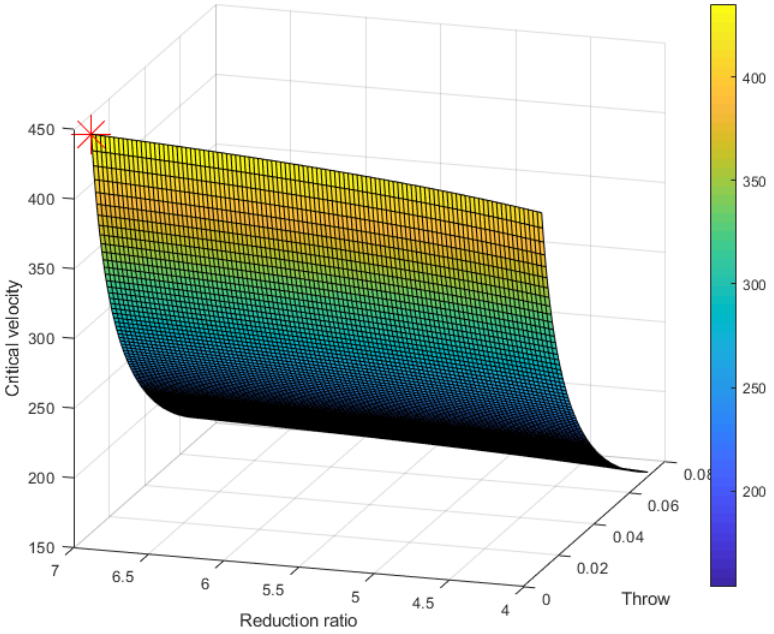

Figure 4.13: Maximum critical velocity

Bond's work index for granite $W_i = 16.59$ kWh/t (Metallurgist 911, 2020),

$f(\beta) = 1$,

$S_C = 1$,

$\rho_s = 2.63$ t/m^3 (Quist, 2012).

The power consumption for scaling factors was obtained and recorded as shown in Table 4.4

Table 4.4: Power consumption for various scaling factors

Scaling Factor	**Power (kWh/t)**
0.5	2.9078
0.6	4.0822
0.7	5.4133
0.8	6.8837
0.9	8.4757
1	10.17

Table 4.4 was used to plot a graph of *Power against Scaling Factor* as shown in Figure 4.14. Using the graph, an equation relating the scaling factor to power consumption was developed:

$$y = 7.086x^2 + 3.845x - 0.743. \tag{4.8}$$

In Equation 4.8, y and x represent the power consumed and scaling factor respectively. The optimal values shown in Table 4.3 were used to calculate the power consumption of the jaw crusher. The power consumed using optimal values was 1.0408 kWh/t and was fed into Equation 4.8 to obtain two roots; 0.299 and -0.8416. The positive roots was taken as the scaling factor. Using a scaling factor of 0.299, a throw of 10 mm, corresponds to 33.445 mm say 35 mm in the full-scale jaw crusher.

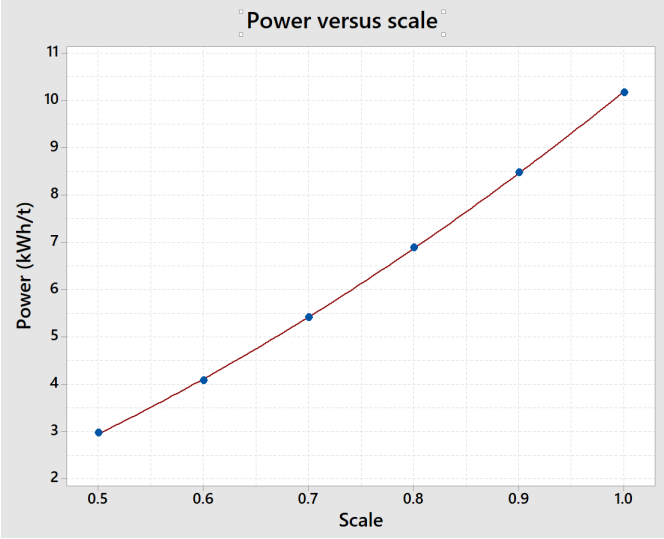

Figure 4.14: Relationship between power and scale factor

Therefore, the optimal operating parameters for a full-size jaw crusher are shown in Table 4.5:

Table 4.5: Optimal operating values for full-size jaw crusher

Parameter	**Optimal Value**
Throw	35 mm
Reduction Ratio	4
Toggle Speed	160 rpm

The operating parameters of the preliminary design of the jaw crusher shown in Figure 1.1 are 35 mm, 3 and 200 rpm for throw, reduction ratio and toggle speed respectively. Using Equation 4.2, the energy efficiency of the unoptimised jaw crusher is 6.023%. The lower efficiency value in the unoptimised jaw crusher was due to the value of reduction ratio of 3. The reduction ratio in the unoptimised jaw crusher is outside the values used in manufacture of jaw crushers and as seen in Figure 4.7, low values of reduction ratio yield low efficiencies.

4.8 Simulation of the Comminution Process

Comminution process is an energy intensive process which requires optimisation. However, during comminution, the feed material interact with the jaw crusher liners leading to wear. The particle flow during comminution also changes as the feed material passes down the crushing chambers. In addition, the rocks interact with the liners during the compression stroke and this affects the rate of wear on the liners. Therefore, even though energy optimisation has been attained, regions experiencing high wear rates and the causes of the wear have not been established.

4.8.1 Behaviour of Particle Flow During Comminution

During the comminution process, there are hundreds of interactions between the particles and the jaw crusher liners. Figure 4.15 (i) shows the particle flow behaviour in a jaw crusher chamber. The BPM rock models are coloured by velocity. It is observed that the velocity varies from zero to a positive value during comminution. When the rock models are squeezed between the liners, the particles in contact with the liners gain velocity as the planes are at an angle as shown in Figure 4.15 (ii) . This implies that the friction between the liners and rock particles influences the flow rate through the crushing chambers. In addition, at the closed set, the particles exit radially and at higher velocity.

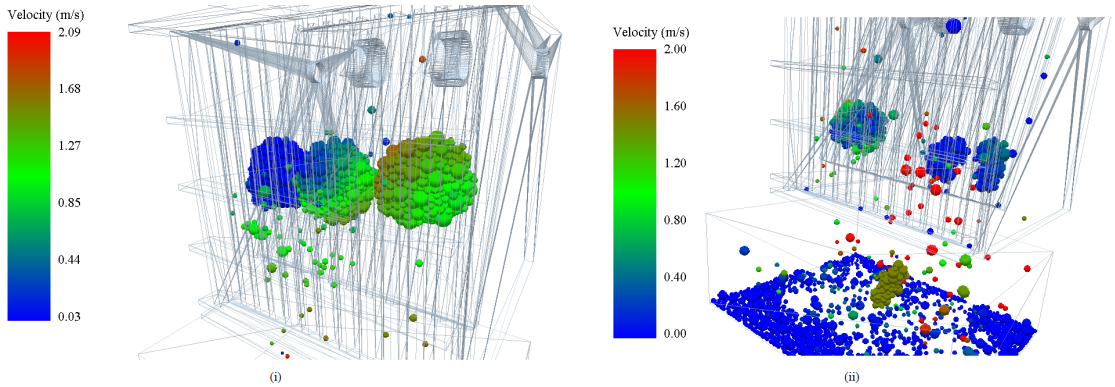

Figure 4.15: Particle flow during comminution:(i) Start of crushing process (ii) End of crushing cycle

4.8.2 Interaction between Jaw Crusher Liners and Rock Model

As the BPM rock model traverses through the crushing chamber, it comes in contact with the jaw crusher liners. It was observed that the rock model experienced loading at different contact points. The number of contact point depended on the shape of the rock. The most common mode of contact was *2-point line and 1-point* as shown by the triangle in Figure 4.16. This was due to the irregular nature of the BPM rock model.

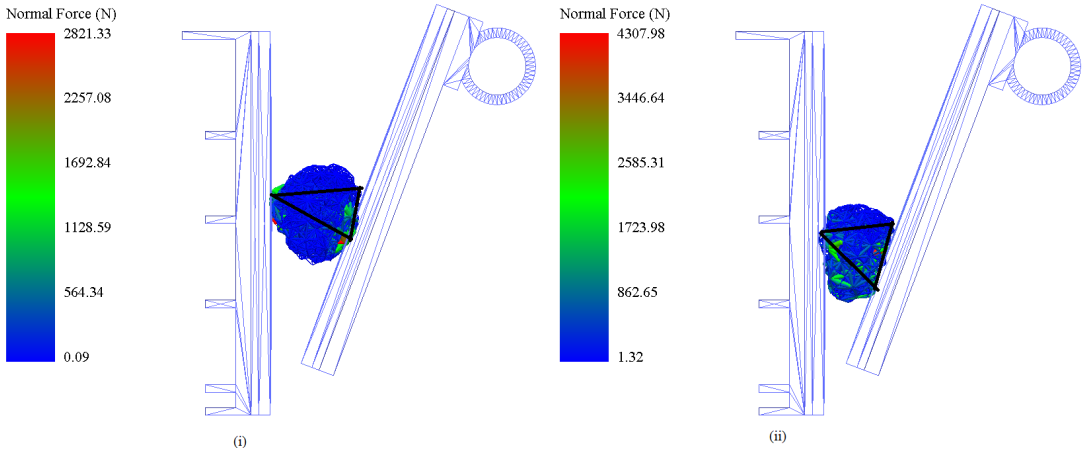

Figure 4.16: Contact points between the rock and jaw crusher liners: (i) Normal forces at start of compression stroke (ii) Normal forces during compression stroke

Maximum compressive forces were present at the contact points and this lead to shatter fracture due to the brittle nature of the rock. The crumbling of the rock at local contact point results in an increment of the contact area and this influences the resultant stresses within the rock and hence the nature of fracture.

In Figure 4.16 (i), the BPM rock model is further away from the CSS than in Figure 4.16 (ii) and this results in a difference of normal forces within the rock. Therefore, the longer the compression stroke the higher the internal stresses within the bonds and hence the higher the probability of fracture. This is why the reduction ratio and throw have a higher impact on total energy efficiency than toggle speed frequency. The high compressive forces within the rock model at the chamber exit result in higher wear rates at the bottom section of the liners.

Energy is usually lost during comminution in form of vibration, noise and heat. However, some energy is also lost as 'stored' energy or residual forces within the crushed material. In Figure 4.17, it is evident that some energy is stored within the BPM rock model during and even after fracture. The energy is indicated by the residual forces within the bonds of the crushed rock. The residual stresses within the

crushed rock at the exit indicate that high magnitudes of compressive forces were required to induce fracture in smaller particles than in large ones as shown in Figure 4.17 (i) and (ii).

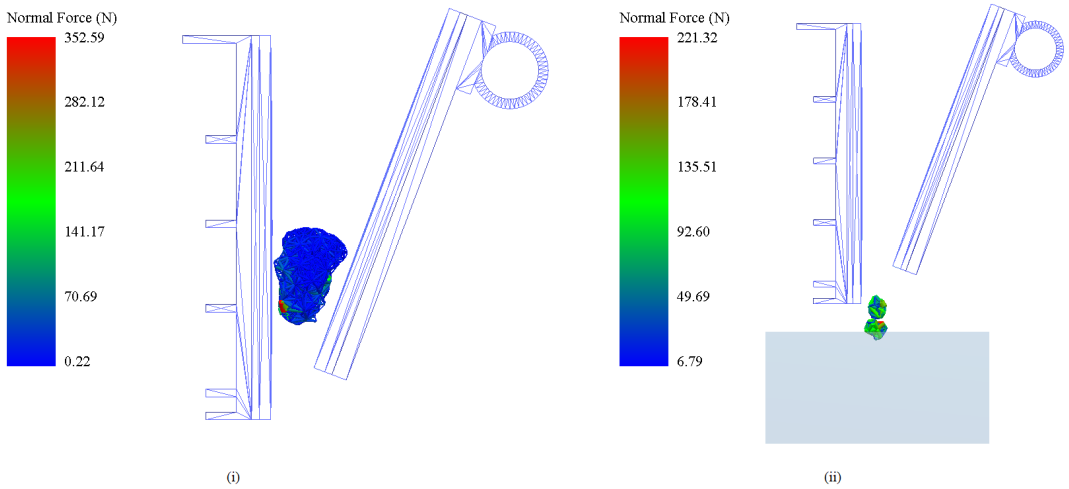

Figure 4.17: Residual forces within the bonds: (i) larger BPM rock model during comminution and (ii) smaller BPM rock model after comminution

4.8.3 Wear Distribution on Jaw Crusher Liners During Comminution

In Figure 4.18, the wear distribution on the liners is depicted by the normal cumulative energy. Energy is released due to friction between the liners and the rocks. In Figure 4.18 (i), the crushing process is still commencing and the maximum normal cumulative energy is 155.48 J. In Figure 4.18 (ii), the size reduction process has ended and the maximum normal cumulative energy increased to 279.54 J. The regions which have not been in contact with the BPM rock model have no wear because they exhibit zero normal cumulative contact energy.

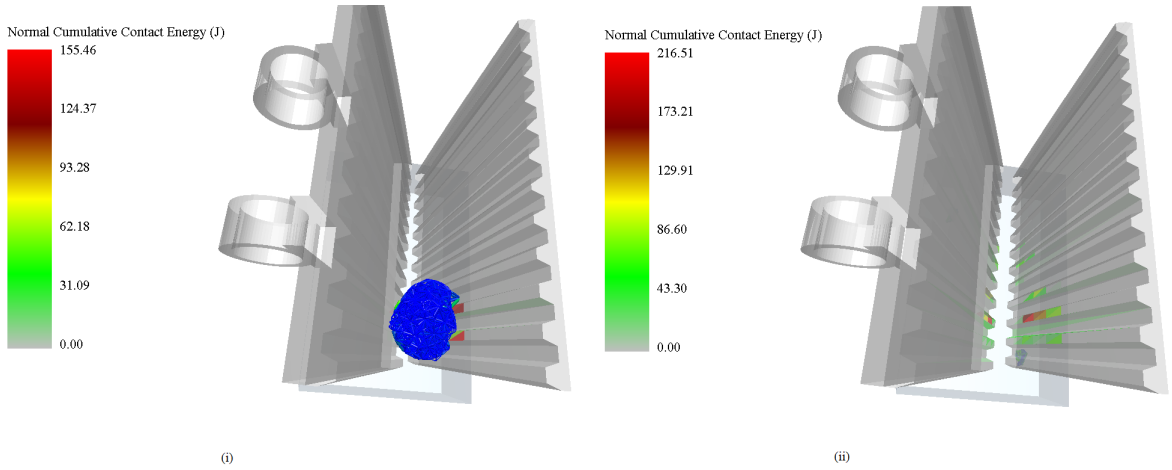

Figure 4.18: Wear distribution on jaw crusher liners at: (i) start of crushing (ii) end of crushing

The highest wear was observed to occur near the close side set (CSS) or the exit of the crusher. In accordance with Weibull's weakest link theory (Khanal, 2005), there is a less probability of formation of critical flaws in a smaller particle than in a larger one. Therefore, since the particle size reduces as it traverses down the crushing chamber, more force is required to induce fracture. Subsequently, as the magnitude of normal forces increase, friction between the BPM rock model and liners increase and hence more wear is experienced near the exit of the crusher. Even though authors have shown that there is wear on the liners using Finite Element Method (Quartey et al., 2017) and experimentally (Lindqvist & Evertsson, 2003), discrete element method has not been used for the analysis in the past. This research has, therefore, filled this gap.

The interaction between the jaw crusher liners in Figure 4.17 shows that the applied normal forces within the BPM rock increase as the particle size gets closer to the exit of the chamber. In addition, due to the high velocities at the exit as the particle flows through the chamber result in high wear rates. This explains why the liners wear more at the close set than at the open set. The high values of exit velocity at the

Closed Side Setting (CSS) were also observed in Quist's research (Quist, 2012). In his research, Quist investigated the wear rate of a cone crusher during comminution. The same behaviour is also observed in the single toggle jaw crusher in which wear rate was more pronounced at the CSS which had not been explained using DEM in previous works.

It is also observed that the fixed jaw liner tended to have more wear than the swing jaw liner. This difference was brought about by the jaw crusher nip angle. The fixed liner is always normal to the rock hence will experience maximum friction force unlike the swing jaw which is inclined. The interaction between the jaw crusher liners in Figure 4.17 shows that the applied normal forces within the BPM rock increase as the particle gets closer to the exit of the chamber.

CHAPTER FIVE

CONCLUSIONS AND RECOMMENDATIONS

5.1 Conclusions

Discrete Element Method was used in modelling of the crushing process taking place in a single toggle jaw crusher. The main aim was to optimise the energy consumption of the comminution process. The total energy efficiency of the crusher was calculated using Equation 4.1. From the results, the following conclusions were made:

i. The total energy efficiency of a single toggle jaw crusher is a function of the throw, reduction ratio and toggle speed. Optimising these operation parameters yielded a jaw crusher whose total energy efficiency was obtained as 60%.

ii. The throw and the reduction ratio had a maximum impact on the total energy efficiency while the toggle speed had the least impact on equipment total energy efficiency.

iii. The wear distribution was established to be more pronounced near the exit of the jaw crusher using DEM.

iv. Based on the Design of Experiments there is a strong interaction between the reduction ratio and the throw. On the contrary, there is minimal interaction between the reduction ratio and toggle speed. This finding is useful as it shows which variables will have a high impact on energy efficiency.

v. A combination of throw and reduction ratio had the highest impact on total energy efficiency while a combination of reduction ratio and toggle speed had

the minimum effect. Therefore, optimising the throw and reduction ratio will have an overall impact on the energy efficiency.

The results obtained from this research will enable manufacturers to design jaw crushers based on the process parameters which have a high impact on energy efficiency i.e. the throw and reduction ratio. In addition, researchers can use the methodology adopted for the energy optimisation process on other comminution machines.

5.2 Recommendations

Based on the results obtained in this research, the following recommendations were made:

i. Due to the high computational power demand by EDEM software, the BPM rock particles were varied between 2 mm and 10 mm in diameter. However, a real rock has particles in ranges of micrometers and it is recommended that finer particles should be used for more realistic predictions.

ii. The motion of the swing jaw was only linear due to the lack of Multi Body Dynamics (MBD) Coupling software in EDEM software. The ideal motion of the swing jaw should be eccentric and this can be achieved using the MBD coupling. It is therefore recommended that the eccentric motion of the swing jaw should be incorporated in future studies. The eccentric motion of the swing jaw will reveal regions exhibiting sliding wear during comminution.

iii. The jaw crusher liner profile used was concave. Use of other profiles such as the Bezier Curve should be investigated using DEM.

iv. Minimisation of wear of the jaw crusher components should be done using DEM. This will increase the life of the liners and enable industries to predict the operation time of liners. Use of custom wear models in EDEM is recommended.

REFERENCES

Abuhasel, K. A. (2019). A Comparative Study of Regression Model and the Adaptive Neuro-Fuzzy Conjecture Systems for Predicting Energy Consumption for Jaw Crusher. *Applied Sciences*, *28*, 766–780.

Amelin, M. (2015). Monte Carlo Simulation in Engineering. Retrieved from `https://www.kth.se/social/files/55e017b4f276545643070e39/MonteCarloSimulationinEngineering.pdf`

Antonyuk, S., Khanal, M., Tomas, J., Heinrich, S., & Mörl, L. (2006). Impact breakage of spherical granules: Experimental study and DEM simulation. *Chemical Engineering and Processing: Process Intensification*, *45*(10), 838–856. doi: 10.1016/j.cep.2005.12.005

Arnold, S. F. (2006). *Design of Experiments with MINITAB* (Vol. 60) (No. 2). doi: 10.1198/tas.2006.s46

Barrios, G., Tavares, L., & Pérez-Prim, J. (2015). DEM Simulation of Bed Particle Compression Using The Particle Replacement Model. *Proceedings of the 14th European Symposium on Comminution and Classification*(September), 59–63.

Barros, A. M., & Lopes, H. S. (2014). *Evolvable Hardware*. doi: 10.4018/978-1-4666-5888-2.ch703

Bazant, Z. P., & Pfeiffer, P. A. (1987). Determination of Fracture Energy From Size Effect and Brittleness Number. *ACI Materials Journal*, *84*(6), 463–480. doi: 10.14359/2526

Brosh, T., Kalman, H., & Levy, A. (2014). Accelerating CFD-DEM simulation of processes with wide particle size distributions. *Particuology*, *12*(1), 113–121. Retrieved from `http://dx.doi.org/10.1016/j.partic.2013.04.008` doi: 10.1016/j.partic.2013.04.008

Cabiscol, R., Finke, J. H., & Kwade, A. (2017). Calibration and interpretation

of DEM parameters for simulations of cylindrical tablets with multi-sphere approach. *Powder Technology*. Retrieved from https://doi.org/10.1016/j.powtec.2017.12.041 doi: 10.1016/j.powtec.2017.12.041

Cabiscol, R., Finke, J. H., Kwade, A., Zheng, W., Tannant, D. D., Zhou, J.-w., ... Djeran-maigre, I. (2017). A discrete element method-based approach to predict the breakage of coal. *Advanced Powder Technology*, *317*(October), 0–1. Retrieved from http://dx.doi.org/10.1016/j.apt.2017.07.019https://doi.org/10.1016/j.ces.2017.12.016http://dx.doi.org/10.1016/j.powtec.2017.05.034http://dx.doi.org/10.1016/j.compgeo.2017.10.004https://doi.org/10.1016/j.powtec.2017.12.041 doi: 10.1016/j.apt.2017.07.019

Cantor, D., Azéma, E., Sornay, P., & Radjai, F. (2017). Three-dimensional bonded-cell model for grain fragmentation. *Computational Particle Mechanics*, *4*(4), 441–450. doi: 10.1007/s40571-016-0129-0

Cho, N. Ã., Martin, C. D., & Sego, D. C. (2007). A clumped particle model for rock. *International Journal of Rock Mechanics and Mining Sciences*, *44*, 997–1010. doi: 10.1016/j.ijrmms.2007.02.002

Cleary, P. W. (2004). Large scale industrial DEM modelling. *Engineering Computations*, *21*(2/3/4), 169–204. Retrieved from http://dx.doi.org/10.1108/02644400410519730 doi: 10.1108/02644400410519730

Cleary, P. W. (2009). Industrial particle flow modelling using discrete element method. *Engineering Computations*, *26*(6), 698–743. doi: 10.1108/02644400910975487

Cleary, P. W., & Morrison, R. D. (2016). Comminution mechanisms, particle shape evolution and collision energy partitioning in tumbling mills. *Minerals Engineering*, *86*, 75–95. Retrieved from http://dx.doi.org/10.1016/j.mineng.2015.12.006 doi: 10.1016/j.mineng.2015.12.006

Cleary, P. W., & Sinnott, M. D. (2015). Simulation of particle flows and breakage in crushers using DEM: Part 1 - Compression crushers. *Minerals Engineering*,

74, 178–197. Retrieved from http://dx.doi.org/10.1016/j.mineng.2014.10.021 doi: 10.1016/j.mineng.2014.10.021

Cleary, P. W., Sinnott, M. D., Morrison, R. D., Cummins, S., & Delaney, G. W. (2017). Analysis of cone crusher performance with changes in material properties and operating conditions using DEM. *Minerals Engineering*, *100*, 49–70. Retrieved from http://dx.doi.org/10.1016/j.mineng.2016.10.005 doi: 10.1016/j.mineng.2016.10.005

Coley, D. (1999). *An introduction to genetic algorithms for scientists and engineers*. Singapore: World Scientific Publishing, Co. Pte. Ltd. doi: 10.1142/3904

Cundall, P. A., & Strack, O. D. L. (1979). A discrete numerical model for granular assemblies. *Géotechnique*, *29*(1), 47–65. doi: 10.1680/geot.1979.29.1.47

Decker, K. M. (1991). The Monte Carlo method in science and engineering: Theory and application. *Computer Methods in Applied Mechanics and Engineering*, *89*(1-3), 463–483. doi: 10.1016/0045-7825(91)90054-A

Deepak, B. (2010). *" Optimum Design and Analysis of Swinging Jaw Plate of a Single Toggle Jaw Crusher "*. Ph. D dessertation, Department of Mechanical Engineering National Institute of Technology, Rourkela.

Delaney, G. W., Morrison, R. D., Sinnott, M. D., Cummins, S., & Cleary, P. W. (2015). DEM modelling of non-spherical particle breakage and flow in an industrial scale cone crusher. *Minerals Engineering*, *74*, 112–122. Retrieved from http://dx.doi.org/10.1016/j.mineng.2015.01.013 doi: 10.1016/j.mineng.2015.01.013

DEM Solutions. (2016). *EDEM 2 . 6 Theory Reference Guide.*

Donovan, J. G. (2003). *Fracture Toughness Based Models for The Prediction of Power Consumption, Product Size, And Capacity of Jaw Crushers*. Blacksburg: Ph. D dessertation, Faculty of the Virginia Polytechnic Institute and State University.

EDEM. (2012). *EDEM 2.4 User Guide.* Retrieved from https://www.edemsimulation.com/

Evertsson, C. M. (1999). Modelling of flow in cone crushers. *Minerals Engineering*, *12*(12), 1479–1499. doi: 10.1016/s0892-6875(99)00136-3

Fuerstenau, D. W., & Abouzeid, A. Z. (2002). The energy efficiency of ball milling in comminution. *International Journal of Mineral Processing*, *67*(1-4), 161–185. doi: 10.1016/S0301-7516(02)00039-X

Garnaik, S. K. (2010). Computer Aided Design of Jaw crusher.

Gu, X., Lu, L., & Qian, J. (2017). Discrete element modeling of the effect of particle size distribution on the small strain stiffness of granular soils. *Particuology*, *32*, 21–29. Retrieved from http://dx.doi.org/10.1016/j.partic.2016.08.002 doi: 10.1016/j.partic.2016.08.002

Gui, N., Yang, X., Tu, J., Jiang, S., & Zhang, Z. (2017). Numerical simulation of tetrahedral particle mixing and motion in rotating drums. *Particuology*. Retrieved from http://dx.doi.org/10.1016/j.partic.2017.08.004 doi: 10.1016/j.partic.2017.08.004

Gupta, A., & Yan, D. (2006). *Mineral processing design and operations: an introduction*. Amsterdam: Elsevier.

Gupta, A., & Yan, D. (2007). *Introduction to Mineral Processing Design and Operation*.

Gupta, M., Alderliesten, R. C., & Benedictus, R. (2015). A review of T-stress and its effects in fracture mechanics. *Engineering Fracture Mechanics*, *134*, 218–241. Retrieved from http://dx.doi.org/10.1016/j.engfracmech.2014.10.013 doi: 10.1016/j.engfracmech.2014.10.013

Han, X. (2014). Investigation of the surface generation mechanism of mechanical polishing engineering ceramics using discrete element method. *Applied Physics A*, *116*(4), 1729–1739. Retrieved from http://link.springer.com/10.1007/s00339-014-8309-3 doi: 10.1007/s00339-014-8309-3

Hoek, E., & Martin, C. D. (2014). Fracture initiation and propagation in intact rock - A review. *Journal of Rock Mechanics and Geotechnical Engineering*, *6*(4), 287–300. Retrieved from http://dx.doi.org/10.1016/j.jrmge.2014

.06.001 doi: 10.1016/j.jrmge.2014.06.001

Hu, G., Otaki, H., & Lin, M. (2001). An index of the tensile strength of brittle particles. *Minerals Engineering*, *14*(10), 1199–1211. doi: 10.1016/S0892-6875(01)00137-6

Hu, J. H. S. X. S. (2015). The role of contact friction in the dynamic breakage behavior of granular materials. doi: 10.1007/s10035-014-0543-z

Industry, N. C. N. (n.d.). *2018 Code of Conduct for Construction Industry.*

Jaeger, B. (2006). The method of least squares. *Handbook of Research on Informatics in Healthcare and Biomedicine*, 181–184. doi: 10.4018/978-1-59140-982-3.ch023

Jeswiet, J., & Szekeres, A. (2016). Energy Consumption in Mining Comminution. *Procedia CIRP*, *48*, 140–145. Retrieved from http://dx.doi.org/10.1016/j.procir.2016.03.250 doi: 10.1016/j.procir.2016.03.250

Jiménez-Herrera, N., Barrios, G. K., & Tavares, L. M. (2017). Comparison of breakage models in DEM in simulating impact on particle beds. *Advanced Powder Technology*, *29*(3), 692–706. doi: 10.1016/j.apt.2017.12.006

Johansson, M., Bengtsson, M., Evertsson, M., & Hulthén, E. (2017). A fundamental model of an industrial-scale jaw crusher. *Minerals Engineering*, *105*, 69–78. Retrieved from http://dx.doi.org/10.1016/j.mineng.2017.01.012 doi: 10.1016/j.mineng.2017.01.012

Kalala, J. T., Bwalya, M. M., & Moys, M. H. (2005). Discrete element method (DEM) modelling of evolving mill liner profiles due to wear. Part I: DEM validation. *Minerals Engineering*, *18*(15), 1386–1391. doi: 10.1016/j.mineng.2005.02.009

Kanda, Y., & Kotake, N. (2007). Comminution Energy and Evaluation in Fine Grinding. *Handbook of Powder Technology*, *12*(07). doi: 10.1016/S0167-3785(07)12015-7

Käsling, H., & Thuro, K. (2010). Determining rock abrasivity in the

laboratory. *Proceedings of the European Rock Mechanics Symposium (EUROCK 2010)*(Figure 1), 1–4. Retrieved from http://lmrwww.epfl.ch/Eurock/Eurock2010/index.htm

Kenya GDP From Construction. (2019). Trading Economics. Retrieved from https://tradingeconomics.com/kenya/gdp-from-construction

Khanal, M. (2005). *Simulation of Crushing Dynamics of an Aggregate-Matrix Composite by Compression and Impact Stressings*. Magdeburg, Germany: Ph. D dessertation, Otto-von-Guericke University of Magdeburg.

Khanal, M., & Jayasundara, C. T. (2014). Role of particle stiffness and inter-particle sliding friction in milling of particles. *Particuology*, *16*, 54–59. Retrieved from http://dx.doi.org/10.1016/j.partic.2014.04.003 doi: 10.1016/j.partic.2014.04.003

Kirankumar, G. (2014). Optimization of Jaw Crusher. , 238–242.

Korman, T., Bedekovic, G., Kujundzic, T., & Kuhinek, D. (2015a). Impact of physical and mechanical properties of rocks on energy consumption of Jaw Crusher. *Physicochemical Problems of Mineral Processing*, *51*(2). doi: 10.5277/ppmp150208

Korman, T., Bedekovic, G., Kujundzic, T., & Kuhinek, D. (2015b). Impact of physical and mechanical properties of rocks on energy consumption of Jaw Crusher. *Physicochemical Problems of Mineral Processing*, *51*(2). doi: 10.5277/ppmp150208

Kwade, A. (2015). Comminution processes : Basics and application to energy efficiency.

LEE, E. (2012). *Optimization of Compressive Crushing*. Goteborg, Sweden: Ph. D dessertation, Department of Product and Production Development, Chalmers University of Technology.

Lee, H., Kwon, J. H., Kim, K. H., & Cho, H. C. (2008). Application of DEM model to breakage and liberation behaviour of recycled aggregates from impact-breakage of concrete waste. *Minerals Engineering*, *21*(11), 761–765. doi: 10.1016/

j.mineng.2008.06.007

Legendre, D., & Zevenhoven, R. (2014). Assessing the energy efficiency of a jaw crusher. *Energy*, *74*, 119–130. doi: 10.1016/j.energy.2014.04.036

Li, H., McDowell, G., & Lowndes, I. (2014). Discrete element modelling of a rock cone crusher. *Powder Technology*, *263*, 151–158. Retrieved from `http://dx.doi.org/10.1016/j.powtec.2014.05.004` doi: 10.1016/j.powtec.2014.05.004

Li, T., Peng, Y., Zhu, Z., Zou, S., & Yin, Z. (2017). Discrete element method simulations of the inter-particle contact parameters for the mono-sized iron ore particles. *Materials*, *10*(5), 19–21. doi: 10.3390/ma10050520

Lichter, J., Lim, K., Potapov, A., & Kaja, D. (2009). New developments in cone crusher performance optimization. *Minerals Engineering*, *22*(7-8), 613–617. Retrieved from `http://dx.doi.org/10.1016/j.mineng.2009.04.003` doi: 10.1016/j.mineng.2009.04.003

Lindqvist, M. (2008). Energy considerations in compressive and impact crushing of rock. *Minerals Engineering*, *21*(9), 631–641. doi: 10.1016/j.mineng.2007.11.013

Lindqvist, M., & Evertsson, C. M. (2003). Linear wear in jaw crushers. *Minerals Engineering*, *16*(1), 1–12. doi: 10.1016/S0892-6875(02)00179-6

Lisjak, A., & Grasselli, G. (2014). A review of discrete modeling techniques for fracturing processes in discontinuous rock masses. *Journal of Rock Mechanics and Geotechnical Engineering*, *6*(4), 301–314. Retrieved from `http://dx.doi.org/10.1016/j.jrmge.2013.12.007` doi: 10.1016/j.jrmge.2013.12.007

Lobo-Guerrero, S., & Vallejo, L. E. (2005). Crushing a weak granular material: experimental numerical analyses. *Géotechnique*, *55*(3), 245–249. doi: 10.1680/geot.2005.55.3.245

Luding, S. (2008). Introduction to discrete element methods: Basic of contact force models and how to perform the micro-macro transition to continuum theory. *European Journal of Environmental and Civil Engineering*, *12*(7-8), 785–826. doi: 10.1080/19648189.2008.9693050

Lusty, P. A. J., & Gunn, A. G. (2015). Challenges to global mineral resource security and options for future supply. *Geological Society, London, Special Publications*, *393*(1), 265–276. Retrieved from http://sp.lyellcollection.org/lookup/doi/10.1144/SP393.13 doi: 10.1144/SP393.13

Magerowski, A. J. (n.d.). Controlling Crushing Costs and Particle Shape.

Marigo, M., & Stitt, E. H. (2015). Discrete element method (DEM) for industrial applications: Comments on calibration and validation for the modelling of cylindrical pellets. *KONA Powder and Particle Journal*, *32*(32), 236–252. doi: 10.14356/kona.2015016

Mas Ivars, D. (2010a). *Bonded Particle Model for Jointed Rock Mass.* Research Gate.

Mas Ivars, D. (2010b). *Bonded particle model for jointed rock mass* (No. January). Retrieved from http://kth.diva-portal.org/smash/record.jsf?pid=diva2:300557

Mcdowell, J. R. (2014). DEM of triaxial tests on crushable sand. , 551–562. doi: 10.1007/s10035-014-0500-x

Metallurgist 911. (2020). *Bond work index tables from various sources.* National Technical Univerity of Athens. Retrieved from https://www.911metallurgist.com/blog/table-of-bond-work-index-by-minerals

Metta, N., Ierapetritou, M., & Ramachandran, R. (2017). A multiscale DEM-PBM approach for a continuous comilling process using a mechanistically developed breakage kernel. *Chemical Engineering Science*. Retrieved from https://doi.org/10.1016/j.ces.2017.12.016 doi: 10.1016/j.ces.2017.12.016

Miller, R. B. (n.d.). *Designing A New Crushing Technique to Combine Impact and Compression Fracturing in A Rock Crushing Chamber.*

Miller, R. O. Y. B. (n.d.). No Title. , 1–14.

Ministry of Mining. (2015). *Kenya Mining Investment Handbook.*

More, R. S., & Raisoni, G. H. (2014). A Design & Analysis of Swing Jaw Plates of Jaw Crusher. *International Journal of Enhanced Research in Science Technology &*

Engineering, *3*(4), 400–408.

Munyasi, M., & Oduori, M. F. (2013). An Overview of the Small Scale Stone Crushing Industry in Western Kenya. In *20th engineers international conference.* Kisumu: Tom Mboya Labour College.

Nader, F., Silvani, C., & Djeran-maigre, I. (2017). Grain breakage under uniaxial compression using a three-dimensional discrete element method. *Granular Matter*, 1–15. doi: 10.1007/s10035-017-0737-2

NCA (National Construction Authority). (2018). *Code of Conduct for the Construction Industry.*

Nezamabadi, S., Nguyen, T. H., Delenne, J. Y., & Radjai, F. (2017). Modeling soft granular materials. *Granular Matter*, *19*(1), 1–12. doi: 10.1007/s10035-016 -0689-y

Numbi, B. P., Zhang, J., & Xia, X. (2014). Optimal energy management for a jaw crushing process in deep mines. *Energy*, *68*, 337–348. Retrieved from `http://dx.doi.org/10.1016/j.energy.2014.02.100` doi: 10.1016/j.energy .2014.02.100

Obermayr, M., Dressler, K., Vrettos, C., & Eberhard, P. (2013). A bonded-particle model for cemented sand. *Computers and Geotechnics*, *49*, 299–313. Retrieved from `http://dx.doi.org/10.1016/j.compgeo.2012.09.001` doi: 10.1016/ j.compgeo.2012.09.001

Olaleye, B. M. (2010). Influence of some rock strength properties on jaw crusher performance in granite quarry. *Mining Science and Technology*, *20*(2), 204–208. Retrieved from `http://dx.doi.org/10.1016/S1674-5264(09) 60185-X` doi: 10.1016/S1674-5264(09)60185-X

Paluszny, A., Tang, X., Nejati, M., & Zimmerman, R. W. (2016). A direct fragmentation method with Weibull function distribution of sizes based on finite- and discrete element simulations. *International Journal of Solids and Structures*, *80*, 38–51. Retrieved from `http://dx.doi.org/10.1016/ j.ijsolstr.2015.10.019` doi: 10.1016/j.ijsolstr.2015.10.019

Park, J. W., & Song, J. J. (2009). Numerical simulation of a direct shear test on a rock joint using a bonded-particle model. *International Journal of Rock Mechanics and Mining Sciences*, *46*(8), 1315–1328. Retrieved from `http://dx.doi.org/10.1016/j.ijrmms.2009.03.007` doi: 10.1016/j.ijrmms.2009.03.007

Pelessone, D., Baum, J. D., Löhner, R., Charman, C. M., & Baylot, J. T. (2003). Convergence study for the discrete particle method. *Computational Fluid and Solid Mechanics 2003*, 2093–2096. doi: 10.1016/B978-008044046-0.50514-5

Potapov, Alexander V., C. S. C. (n.d.). A three dimensional simulation of brittle solid fracture. *International Journal of Modern Physics*, *Volume 7*(No. 5).

Potyondy, D. O., & Cundall, P. A. (2004). A bonded-particle model for rock. *International Journal of Rock Mechanics and Mining Sciences*, *41*(8 SPEC.ISS.), 1329–1364. doi: 10.1016/j.ijrmms.2004.09.011

Quartey, G., Njoroge, K., & Kihiu, J. M. (2017). Study on Liner wear in Single Toggle Jaw Crushers: A Review. *JSRE*, *8*(6), 1646–1650.

Quist, J. (2012). *Cone Crusher Modelling and Simulation using DEM* (No. 1652). Goteborg, Sweden: Ph. D desssertation, Chalmers University of Technology. doi: 10.1016/j.mineng.2015.11.004

Radziszewski, P. (2013). Energy recovery potential in comminution processes. *Minerals Engineering*, *46-47*, 83–88. Retrieved from `http://dx.doi.org/10.1016/j.mineng.2012.12.002` doi: 10.1016/j.mineng.2012.12.002

Rafidah, A., Nurulhuda, A., Azrina, A., Suhaila, Y., Anwar, I. S., & Syafiq, R. A. (2014). Comparison design of experiment (DOE): Taguchi method and full factorial design in surface roughness. *Applied Mechanics and Materials*, *660*(October), 275–279. doi: 10.4028/www.scientific.net/AMM.660.275

Ramalho, A., & Miranda, J. C. (2006). The relationship between wear and dissipated energy in sliding systems. *Wear*, *260*(4-5), 361–367. doi: 10.1016/j.wear.2005.02.121

Rashidi Moghaddam, M., Ayatollahi, M., Razavi, S., & Berto, F. (2017). Mode

II Brittle Fracture Assessment Using an Energy Based Criterion. *Physical Mesomechanics*, *20*(2), In Press. doi: 10.1134/S1029959917020047

Refahi, A., Mohandesi, J. A., & Rezai, B. (2010). International Journal of Mineral Processing Discrete element modeling for predicting breakage behavior and fracture energy of a single particle in a jaw crusher. *International Journal of Mineral Processing*, *94*(1-2), 83–91. doi: 10.1016/j.minpro.2009.12.002

Rojas, E., Vergara, V., & Soto, R. (2019). Case study: Discrete element modeling of wear in mining hoppers. *Wear*, *430-431*(April), 120–125. Retrieved from https://doi.org/10.1016/j.wear.2019.04.020 doi: 10.1016/j.wear.2019.04.020

Rosales-Marín, G., Andrade, J., Alvarado, G., Delgadillo, J. A., & Tuzcu, E. T. (2019). Study of lifter wear and breakage rates for different lifter geometries in tumbling mill: Experimental and simulation analysis using population balance model. *Minerals Engineering*, *141*(June), 105857. Retrieved from https://doi.org/10.1016/j.mineng.2019.105857 doi: 10.1016/j.mineng.2019.105857

Roylance, D. (2001). Introduction to Fracture Mechanics. , 1–17.

Rumpf, H. (1975). Particle Technology. *Particle Technology Series*. Retrieved from https://books.google.fr/books?id=GI3tCAAAQBAJ doi: 10.1007/978-94-011-7944-7

Russell, A. R., Muir Wood, D., & Kikumoto, M. (2009). Crushing of particles in idealised granular assemblies. *Journal of the Mechanics and Physics of Solids*, *57*(8), 1293–1313. Retrieved from http://dx.doi.org/10.1016/j.jmps.2009.04.009 doi: 10.1016/j.jmps.2009.04.009

Schroe, K. (2016). Production, Handling and Characterization of Particulate Materials. In *Production, handling and characterization of particulate materials* (Vol. 25, pp. 257 – 289). Springer. Retrieved from http://link.springer.com/10.1007/978-3-319-20949-4 doi: 10.1007/978-3-319-20949-4

Schubert, W. (2005). DEM Simulation of the Breakage Process in an Impact Crusher.

Granular Matter, *4*, 1–8. Retrieved from www.uni-magdeburg.de

Shrivastava, A. K., & Sharma, A. (2012). A review on study of jaw crusher. *International Journal of Modern Engineering Research*, *2*(3), 885–888.

Smith, R. L., Mecholsky, J. J., & Freiman, S. W. (2009). Estimation of fracture energy from the work of fracture and fracture surface area: I. Stable crack growth. *International Journal of Fracture*, *156*(1), 97–102. doi: 10.1007/s10704-009-9350-7

Spall, J. C. (1999). Overview of the simultaneous perturbation method for efficient optimization. *American Society of Civil Engineers - Task Committee Reports*, *19*(4), 141–154.

Spettl, A., Dosta, M., Antonyuk, S., Heinrich, S., & Schmidt, V. (2015). Statistical investigation of agglomerate breakage based on combined stochastic microstructure modeling and DEM simulations. *Advanced Powder Technology*, *26*(3), 1021–1030. Retrieved from http://dx.doi.org/10.1016/j.apt.2015.04.011 doi: 10.1016/j.apt.2015.04.011

Sprunt, S. (2000). Technical Note Real-time SEM Observations of the Microfracturing Process in Rock During a Compression Test. *International Journal of Rock Mechanics and Mining Sciences & Geomechanics Abstracts*, *30*(6), 643–652.

Sundar.V, S. (2014). Optimum design and analysis of single toggle jaw crusher. , *8354*(3), 194–203.

Suresh, B. A. (2009). *" Computer Aided Design and Analysis of Swing Jaw Plate of Jaw Crusher "*. Ph. D dessertation, Department of Mechanical Engineering National Institute of Technology, Rourkela.

Tapponnier, P., & Bracet, W. F. (1976). Development.of Stress-Induced Microcracks m Westerly Granite. *Int. J. Rock Mech. Min. Sci. & Geomech. Abstr*, *13*, 103–112.

Timoshenko, S., & Goodier, J. N. (1951). *Theory of elasticity, 2nd edition.* doi: 10.1007/BF00046464

Tromans, D. (2008). Mineral comminution: Energy efficiency considerations. *Minerals Engineering*, *21*(8), 613–620. doi: 10.1016/j.mineng.2007.12.003

Tromans, D., & Meech, J. A. (2002). Fracture toughness and surface energies of minerals: theoretical estimates for oxides, sulphides, silicates and halides. *Minerals Engineering*, *17*(1), 1–15. doi: 10.1016/j.mineng.2003.09.006

Tromans, D., & Meech, J. A. (2004). Fracture toughness and surface energies of covalent minerals: Theoretical estimates. *Minerals Engineering*, *17*(1), 1–15. doi: 10.1016/j.mineng.2003.09.006

Vallet, D., & Charmet, J. C. (1995). Mechanical behaviour of brittle cement grains. *Journal of Materials Science*, *30*(11), 2962–2967. doi: 10.1007/BF00349670

Venter, G. (2010). Review of Optimization Techniques. *Encyclopedia of Aerospace Engineering*, 1–12. doi: 10.1002/9780470686652.eae495

Vogel, L., & Peukert, W. (2005). From single particle impact behaviour to modelling of impact mills. *Chemical Engineering Science*, *60*(18), 5164–5176. doi: 10 .1016/j.ces.2005.03.064

Wang, B., Martin, U., & Rapp, S. (2017). Discrete element modeling of the single-particle crushing test for ballast stones. *Computers and Geotechnics*, *88*, 61–73. Retrieved from `http://dx.doi.org/10.1016/j.compgeo.2017.03.007` doi: 10.1016/j.compgeo.2017.03.007

Wang, P., & Arson, C. (2016). Discrete element modeling of shielding and size effects during single particle crushing. *Computers and Geotechnics*, *78*, 227–236. Retrieved from `http://dx.doi.org/10.1016/j.compgeo.2016.04.003` doi: 10.1016/j.compgeo.2016.04.003

Wanne, T. S., & Young, R. P. (2008). Bonded-particle modeling of thermally fractured granite. *International Journal of Rock Mechanics and Mining Sciences*, *45*(5), 789–799. doi: 10.1016/j.ijrmms.2007.09.004

Weerasekara, N. S., Powell, M. S., Cleary, P. W., Tavares, L. M., Evertsson, M., Morrison, R. D., ... Carvalho, R. M. (2013). The contribution of DEM to the science of comminution. *Powder Technology*, *248*, 3–4. Retrieved from `http://`

dx.doi.org/10.1016/j.powtec.2013.05.032 doi: 10.1016/j.powtec.2013.05.032

Weng, M. C., & Li, H. H. (2012). Relationship between the deformation characteristics and microscopic properties of sandstone explored by the bonded-particle model. *International Journal of Rock Mechanics and Mining Sciences*, *56*, 34–43. Retrieved from http://dx.doi.org/10.1016/j.ijrmms.2012.07.003 doi: 10.1016/j.ijrmms.2012.07.003

Wong, K. V. (2007). *Thermodynamics for Engineers* (Second Edi ed., Vol. 134) (No. 4). London.

Wong, L. N. Y., & Li, H. Q. (2013). Numerical study on coalescence of two pre-existing coplanar flaws in rock. *International Journal of Solids and Structures*, *50*(22-23), 3685–3706. Retrieved from http://dx.doi.org/10.1016/j.ijsolstr.2013.07.010 doi: 10.1016/j.ijsolstr.2013.07.010

Wu, C. L., Ayeni, O., Berrouk, A. S., & Nandakumar, K. (2014). Parallel algorithms for CFD-DEM modeling of dense particulate flows. *Chemical Engineering Science*, *118*, 221–244. doi: 10.1016/j.ces.2014.07.043

Xu, L., Luo, K., & Zhao, Y. (2018). Numerical prediction of wear in SAG mills based on DEM simulations. *Powder Technology*, *329*, 353–363. Retrieved from https://doi.org/10.1016/j.powtec.2018.02.004 doi: 10.1016/j.powtec.2018.02.004

Y. Nakata, A. F. Hyde, H. M. (1999). A probabilistic approach to sand particle crushing in the triaxial test. (5), 567–583.

Yashima, S., Kanda, Y., & National, Z. (1987). Relationships Between Particle Size and Fracture Energy or Impact Velocity Required to Fracture as Estimated from Single Particle Crushing. , *51*, 277–282.

Zhang, Z. X. (2016). Rock Fracture and Rock Strength. *Rock Fracture and Blasting*, 69–88. doi: 10.1016/b978-0-12-802688-5.00003-8

Zhao, T. (2017). Coupled DEM-CFD analyses of landslide-induced debris flows. In *Analyses of landslide-induced debris flows* (pp. 25–45). Singapore: Springer.

doi: 10.1007/978-981-10-4627-8

Zheng, W., & Tannant, D. D. (2017). Computers and Geotechnics Grain breakage criteria for discrete element models of sand crushing under one-dimensional compression. *Computers and Geotechnics*(October), 0–1. Retrieved from http://dx.doi.org/10.1016/j.compgeo.2017.10.004 doi: 10.1016/j.compgeo.2017.10.004

Zhou, J.-w., Liu, Y., Du, C.-l., & Liu, S.-y. (2017). Effect of the particle shape and swirling intensity on the breakage of lump coal particle in pneumatic conveying. *Powder Technology*, *317*, 438–448. Retrieved from http://dx.doi.org/10.1016/j.powtec.2017.05.034 doi: 10.1016/j.powtec.2017.05.034

Appendices

APPENDIX A

Genetic Algorithm

```
%objective function used in GA
function N= N_energy_Uc(x)
N=(188.5-0.3709.*x(3)-19.51.*x(2)-7.431.*x(1)+0.04099.*x(3).*x(2)
+0.01629.*x(3).*x(1)+1.066.*x(1).*x(2)-0.001916.*x(1).*x(2).*x(3));
end
```

Figure A.1: Objective function used in optimisation

```
%Genetic algorithm code
Lb = [0.01 4 100];%Lower bound limit
Ub = [0.035 7 300];%Upper bound limit
nvar = 3;
fitnessF = @(x) N_energy_Uc(x);%calling the objective function
opt= optimoptions('ga', 'Display', 'iter',... %Displays the iterations
    'MaxGeneration', 1000*nvar,... %Defines the number of generations %increasing improves accuracy
    'PopulationSize', 500,... %sets the populationsize
    'FunctionTolerance', 1e-6,... %this is the function tolerance %reducing improves accuracy
    'PlotFcn', @gaplotbestindiv); %This command visualizes the results
[x, fval]=ga(fitnessF,nvar, [], [], [], [], Lb, Ub, [], opt);
```

Figure A.2: Genetic algorithm code

APPENDIX B

EDEM C++ Custom API Files

```
ParticleReplace: Whole
ParticleCluster: Fraction
StartBondingTime: 0.1
```

Figure B.1: Particle replacement preference file

```
using namespace std;
using namespace NApi;
using namespace NApiCore;
using namespace NApiPbf;

//Add the name for the preference file
const string CCustomParticleBodyForce::PREFS_FILE = "Particle_Replacement_prefs.txt";
```

Figure B.2: Calling *ParticleReplacementprefs.txt* in C++ custom factory API code

```
764
0.00364581      -0.00555962     0.00959717      5
0.00415037      -0.00938728     -0.0211683      2.4985
-0.0129888      0.008434        0.000445034     4.121655
-0.0251761      0.00385112      0.0143717       5
0.0117001       0.008212        -0.00480682     5
0.0168851       -0.0161447      0.013619        5
0.0270869       0.0133378       -0.0057265      5
-0.00188411     -0.00966319     0.00152586      5
-0.0144866      0.00544685      -0.0147846      5
0.025539        0.00601701      0.00709333      3.543015
0.0149247       0.0141397       -0.00257003     2.10926
0.0119049       -0.00411582     -0.00441376     2.9763
0.0173088       0.0110426       0.0140314       3.66066
-0.00179461     -0.0149534      -0.0127986      5
0.00965067      -0.012049       -0.00343943     5
0.0260984       0.00547001      0.00106425      2.524315
-0.00125574     -0.00894126     -0.00573629     2.017615
-0.00077236     0.0360701       -0.00610688     5
```

Figure B.3: Cluster data file showing particle positions and scaling factor in BPM rock model